

# *Uniform enclosures for the phase and zeros of Bessel functions and their derivatives*

Article

Accepted Version

Creative Commons: Attribution 4.0 (CC-BY)

Filonov, N., Levitin, M. ORCID: <https://orcid.org/0000-0003-0020-3265>, Polterovich, I. and Sher, D. A. (2024) Uniform enclosures for the phase and zeros of Bessel functions and their derivatives. *SIAM Journal on Mathematical Analysis* (SIMA), 56 (6). pp. 7644-7682. ISSN 1095-7154 doi: <https://doi.org/10.1137/24M1642032> Available at <https://centaur.reading.ac.uk/117826/>

It is advisable to refer to the publisher's version if you intend to cite from the work. See [Guidance on citing](#).

To link to this article DOI: <http://dx.doi.org/10.1137/24M1642032>

Publisher: Society for Industrial and Applied Mathematics

All outputs in CentAUR are protected by Intellectual Property Rights law, including copyright law. Copyright and IPR is retained by the creators or other copyright holders. Terms and conditions for use of this material are defined in the [End User Agreement](#).

[www.reading.ac.uk/centaur](http://www.reading.ac.uk/centaur)

**CentAUR**

Central Archive at the University of Reading

Reading's research outputs online

# Uniform enclosures for the phase and zeros of Bessel functions and their derivatives

Nikolay Filonov

Michael Levitin

Iosif Polterovich

David A. Sher

arXiv:2402.06956v3; 16 July 2024

## Abstract

We prove explicit uniform two-sided bounds for the phase functions of Bessel functions and of their derivatives. As a consequence, we obtain new enclosures for the zeros of Bessel functions and their derivatives in terms of inverse values of some elementary functions. These bounds are valid, with a few exceptions, for all zeros and all Bessel functions with non-negative indices. We provide numerical evidence showing that our bounds either improve or closely match the best previously known ones.

## Contents

|          |                                                                                            |           |
|----------|--------------------------------------------------------------------------------------------|-----------|
| <b>1</b> | <b>Introduction and main results</b>                                                       | <b>2</b>  |
| 1.1      | Setup I: Bessel functions . . . . .                                                        | 2         |
| 1.2      | Setup II: derivatives of Bessel functions . . . . .                                        | 4         |
| 1.3      | Our philosophy and some history . . . . .                                                  | 6         |
| 1.4      | Definitions and properties of the auxiliary functions I . . . . .                          | 7         |
| 1.5      | Main results I: bounding the phase and zeros of Bessel functions . . . . .                 | 8         |
| 1.6      | Definitions and properties of the auxiliary functions II . . . . .                         | 10        |
| 1.7      | Main results II: bounding the phase and zeros of derivatives of Bessel functions . . . . . | 11        |
| <b>2</b> | <b>Proofs</b>                                                                              | <b>13</b> |
| 2.1      | Liouville's transformation and phase functions . . . . .                                   | 13        |
| 2.2      | A consequence of the Sturm comparison theorem . . . . .                                    | 14        |
| 2.3      | Proof of Theorem 1.4 . . . . .                                                             | 15        |
| 2.4      | Proof of Lemma 1.8 . . . . .                                                               | 16        |
| 2.5      | Proof of Theorem 1.10 . . . . .                                                            | 17        |

---

The accompanying `Mathematica` script and its printout are available for download at <https://michaellevitin.net/bessels.html>.

**MSC(2020):** Primary 33C10. Secondary 33F05, 34B30, 65D20.

**Keywords:** Bessel functions, Bessel zeros, phase function, Sturm oscillation theorem, one-dimensional Schrödinger equation

**N. F.:** St. Petersburg Department of Steklov Institute of Mathematics of RAS, Fontanka 27, 191023, St.Petersburg, Russia; St. Petersburg State University, University emb. 7/9, 199034, St.Petersburg, Russia; [filonov@pdmi.ras.ru](mailto:filonov@pdmi.ras.ru)

**M. L.:** Department of Mathematics and Statistics, University of Reading, Pepper Lane, Whiteknights, Reading RG6 6AX, UK; [M.Levitin@reading.ac.uk](mailto:M.Levitin@reading.ac.uk); <https://www.michaellevitin.net>

**I. P.:** Département de mathématiques et de statistique, Université de Montréal, CP 6128 succ Centre-Ville, Montréal QC H3C 3J7, Canada; [iossif@dms.umontreal.ca](mailto:iossif@dms.umontreal.ca); <https://www.dms.umontreal.ca/~iossif>

**D. A. S.:** Department of Mathematical Sciences, DePaul University, 2320 N. Kenmore Ave, 60614, Chicago, IL, USA; [dsher@depaul.edu](mailto:dsher@depaul.edu)

|          |                                                                                                  |           |
|----------|--------------------------------------------------------------------------------------------------|-----------|
| <b>3</b> | <b>Derivatives of ultraspherical Bessel functions</b>                                            | <b>19</b> |
| 3.1      | Setup III                                                                                        | 19        |
| 3.2      | Phase function of ultraspherical Bessel derivatives                                              | 20        |
| 3.3      | Definitions and properties of the auxiliary functions III                                        | 22        |
| 3.4      | Main results III: bounding the phase and zeros of derivatives of ultraspherical Bessel functions | 23        |
| <b>4</b> | <b>Benchmarking and conclusions</b>                                                              | <b>25</b> |
|          | <b>Acknowledgements</b>                                                                          | <b>26</b> |
|          | <b>References</b>                                                                                | <b>27</b> |
| <b>A</b> | <b>Explicit expressions for some potentials</b>                                                  | <b>28</b> |
| <b>B</b> | <b>Numerical data</b>                                                                            | <b>30</b> |
| B.1      | Bounds for zeros of Bessel functions                                                             | 30        |
| B.2      | Bounds for zeros of derivatives of Bessel functions                                              | 35        |

## §I. Introduction and main results

### §I.1. Setup I: Bessel functions

Throughout,

$$J_\nu(x), \quad Y_\nu(x)$$

are standard Bessel functions with  $\nu \geq 0$ , and

$$j_{\nu,k}, \quad y_{\nu,k}$$

are their  $k$ th largest positive zeros, respectively, where  $k \in \mathbb{N}$ .

We further define

$$\mathcal{C}_{\nu,\tau}(x) := J_\nu(x) \cos(\pi\tau) + Y_\nu(x) \sin(\pi\tau),$$

where we choose the additional parameter  $\tau \in (0, 1]$  for definiteness, see Figure 1. Note that

$$J_\nu(x) = -\mathcal{C}_{\nu,1}(x), \quad Y_\nu(x) = \mathcal{C}_{\nu,\frac{1}{2}}(x).$$

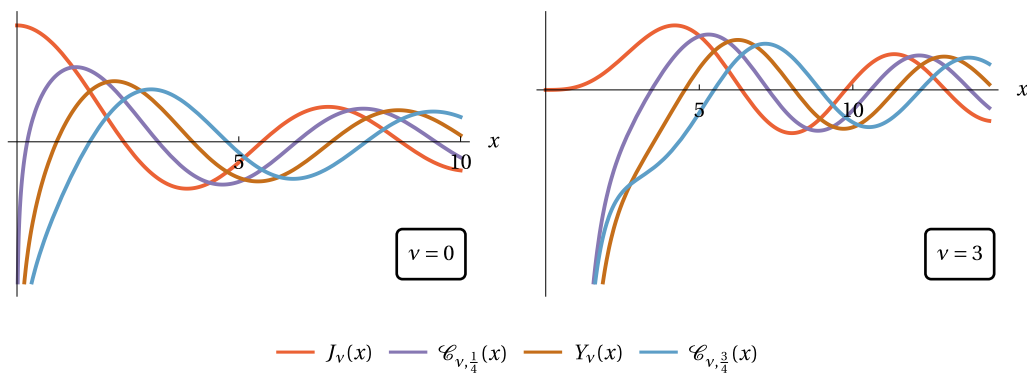


**Figure 1:** Plots of  $\mathcal{C}_{\nu,\tau}(x)$ .

We also introduce the Bessel *modulus* and *phase functions*  $M_\nu, \theta_\nu : (0, +\infty) \rightarrow \mathbb{R}$  defined by

$$M_\nu(x) = \sqrt{J_\nu^2(x) + Y_\nu^2(x)}, \quad J_\nu(x) + iY_\nu(x) = M_\nu(x) (\cos \theta_\nu(x) + i \sin \theta_\nu(x)),$$

where we choose a continuous branch of  $\theta_\nu(x)$  with the initial condition

$$\lim_{x \rightarrow 0^+} \theta_\nu(x) = -\frac{\pi}{2}.$$

For more details on the modulus and phase functions see [DLMF, §10.18] and [Hor7].

The following properties of the Bessel zeros and the modulus and phase functions are standard. We have

$$\nu < y_{\nu,1} < j_{\nu,1} < y_{\nu,2} < j_{\nu,2} < \dots < y_{\nu,k} < j_{\nu,k} < \dots,$$

see also [Pan] for further interlacing properties. Also,

$$M_\nu(x) > 0, \quad \theta'_\nu(x) > 0 \quad \text{for all } x > 0,$$

which means that the inverse function

$$\theta_\nu^{-1} : \left[-\frac{\pi}{2}, +\infty\right) \rightarrow [0, +\infty)$$

is well-defined and continuous. We also have, by [DLMF, (10.18.18)], the asymptotics

$$\theta_\nu(x) = x - \frac{\pi}{4}(2\nu + 1) + \frac{4\nu^2 - 1}{8x} + \frac{(4\nu^2 - 1)(4\nu^2 - 25)}{384x^3} + O(x^{-5}) \quad \text{as } x \rightarrow +\infty. \quad (1.1)$$

We have, since  $j_{\nu,k}$  are the positive zeros of  $\cos \theta_\nu(x)$ , and  $y_{\nu,k}$  are the positive zeros of  $\sin \theta_\nu(x)$ , the relations

$$j_{\nu,k} = \theta_\nu^{-1} \left( \pi \left( k - \frac{1}{2} \right) \right), \quad y_{\nu,k} = \theta_\nu^{-1} (\pi (k - 1)), \quad k \in \mathbb{N}. \quad (1.2)$$

Some typical plots of functions  $\theta_\nu$  are shown in Figure 2.

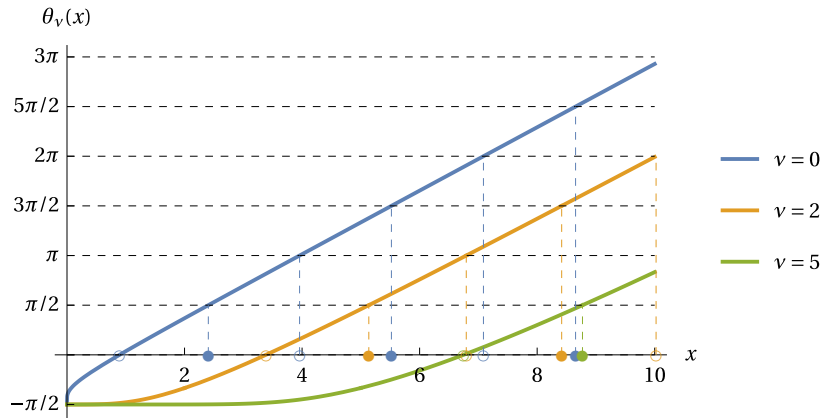


**Figure 2:** Plots of  $\theta_\nu(x)$ . The filled colour-coded dots on the horizontal axis indicate the positions of zeros  $j_{\nu,k}$  and the hollow dots the positions of zeros  $y_{\nu,k}$ . The phase functions are calculated using the method of [Hor7].

We also have

$$\mathcal{C}_{\nu,\tau}(x) = M_\nu(x) \cos(\theta_\nu(x) - \pi\tau).$$

The  $k$ th positive zero of this function, which we will denote by  $c_{\nu,\tau,k}$ , is given by

$$c_{\nu,\tau,k} = \theta_\nu^{-1} \left( \pi \left( \tau + k - \frac{3}{2} \right) \right). \quad (1.3)$$

*Remark 1.1.* We know that the first zero of either  $J_\nu(x)$  or  $Y_\nu(x)$  is always bigger than  $\nu$ . This is not necessarily the case for  $c_{\nu,\tau,1}$  with  $\tau \in (0, \frac{1}{2})$ . Indeed, we have

$$c_{\nu,\tau,1} = \theta_\nu^{-1} \left( \pi \left( \tau - \frac{1}{2} \right) \right) \leq \nu$$

whenever

$$0 < \tau \leq \tau_\nu^* := \frac{1}{\pi} \theta_\nu(\nu) + \frac{1}{2}.$$

Since  $\theta_\nu(\nu) \in [-\frac{\pi}{2}, 0)$ , we always have  $\tau_\nu^* \in [0, \frac{1}{2})$ , see Figure 3. ◀

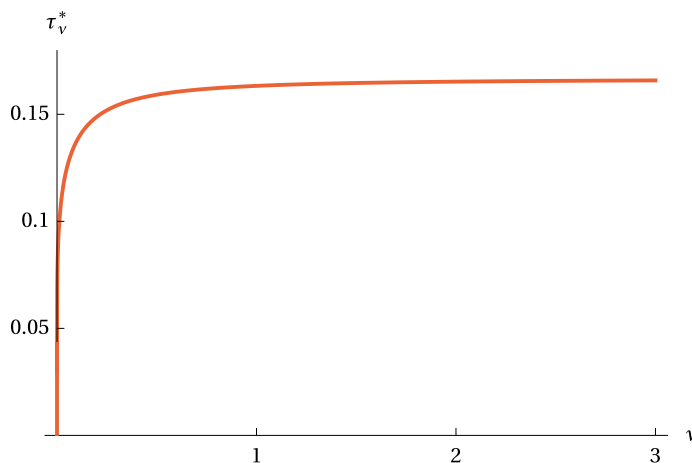


**Figure 3:** Plot of  $\tau_\nu^*$  against  $\nu$ .

For further use, we additionally define the *counting function* of Bessel zeros,

$$\mathcal{N}_{J_\nu}(\lambda) := \#\{k \in \mathbb{N} : j_{\nu,k} \leq \lambda\}. \quad (1.4)$$

### §1.2. Setup II: derivatives of Bessel functions

Consider, for  $\nu \geq 0$ , the derivatives of the Bessel functions

$$J'_\nu(x), \quad Y'_\nu(x).$$

The numbers

$$j'_{\nu,k}, \quad y'_{\nu,k}$$

are their  $k$ th largest positive zeros except when  $\nu = 0$ , in which case we set

$$j'_{0,1} := 0.$$

We also consider the linear combinations

$$\mathcal{C}'_{\nu,\tau}(x) := J'_\nu(x) \cos(\pi\tau) + Y'_\nu(x) \sin(\pi\tau),$$

this time with  $\tau \in [0, 1)$ , see Figure 4.

As for the Bessel functions themselves, we also introduce the *modulus* and *phase functions* of the Bessel derivatives,  $N_\nu, \varphi_\nu : (0, +\infty) \rightarrow \mathbb{R}$  defined by

$$N_\nu(x) = \sqrt{(J'_\nu(x))^2 + (Y'_\nu(x))^2}, \quad J'_\nu(x) + iY'_\nu(x) = N_\nu(x) (\cos \varphi_\nu(x) + i \sin \varphi_\nu(x)),$$

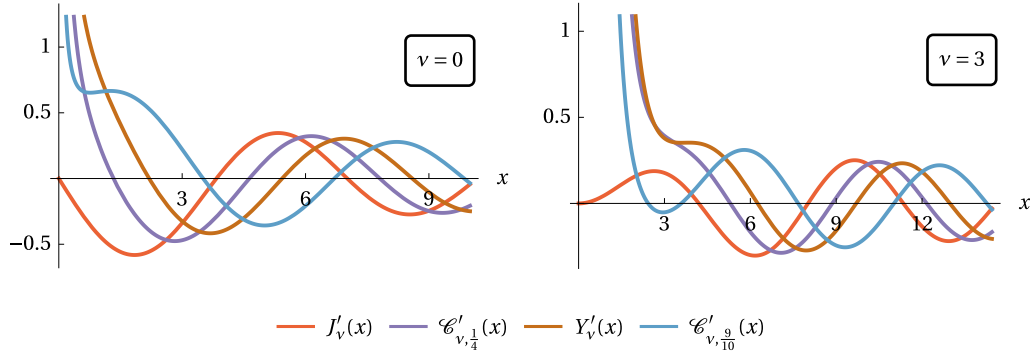


Figure 4: Plots of  $\mathcal{C}'_{v,\tau}(x)$ .

where we choose a continuous branch of  $\varphi_\nu(x)$  with the initial condition

$$\lim_{x \rightarrow 0^+} \varphi_\nu(x) = \frac{\pi}{2},$$

see [DLMF, §10.18] and [Ho17].

The following properties of the Bessel derivatives zeros and the modulus and phase functions are standard:

$$\nu \leq j'_{\nu,1} < y'_{\nu,1} < j'_{\nu,2} < y'_{\nu,2} < \dots < j'_{\nu,k} < y'_{\nu,k} < \dots$$

(with equality only for  $\nu = 0$ );

$$N_\nu(x) > 0 \quad \text{for all } x > 0.$$

The phase function  $\varphi_\nu$  is not monotone (except for  $\nu = 0$ ) but has a single minimum at  $x = \nu$ , with  $\varphi_\nu(\nu) \in (0, \frac{\pi}{2})$  for  $\nu > 0$ . This means that its inverse function may only be defined on  $[\varphi_\nu(\nu), +\infty)$ ; it is however easier to further restrict its domain and treat it as the function

$$\varphi_\nu^{-1} : \left[ \frac{\pi}{2}, +\infty \right) \rightarrow [j'_{\nu,1}, +\infty).$$

Additionally, by [DLMF, (10.18.21)],

$$\varphi_\nu(x) = x - \frac{\pi}{4}(2\nu + 1) + \frac{4\nu^2 + 3}{8x} + \frac{16\nu^4 + 184\nu^2 - 63}{384x^3} + O(x^{-5}) \quad \text{as } x \rightarrow +\infty. \quad (1.5)$$

We have

$$j'_{\nu,k} = \varphi_\nu^{-1} \left( \pi \left( k - \frac{1}{2} \right) \right), \quad y'_{\nu,k} = \varphi_\nu^{-1}(\pi k), \quad k \in \mathbb{N}. \quad (1.6)$$

Further, let

$$c'_{\nu,\tau,k} := \varphi_\nu^{-1} \left( \pi \left( \tau + k - \frac{1}{2} \right) \right), \quad k \in \mathbb{N}, \quad (1.7)$$

be the  $k$ th largest zero of

$$\mathcal{C}'_{\nu,\tau}(x) = N_\nu(x) \cos(\varphi_\nu(x) - \pi\tau).$$

in the interval  $[j'_{\nu,1}, +\infty)$ .

**Example 1.2.** Our choice of enumeration of  $c'_{\nu,\tau,k}$  means that we may disregard some positive zeros of  $\mathcal{C}'_{\nu,\tau}$  below  $j'_{\nu,1}$ . For example, the right-hand side plot in Figure 4 shows that there are two zeros of  $\mathcal{C}'_{3,\frac{9}{10}}$  below the first zero of  $J'_3$ , which are therefore excluded. ◀

Some typical plots of functions  $\varphi_\nu$  are shown in Figure 5.

Similarly to (1.4), we also define the *counting function* of zeros of Bessel derivatives,

$$\mathcal{N}_{J'_\nu}(\lambda) := \# \left\{ k \in \mathbb{N} : j'_{\nu,k} \leq \lambda \right\}. \quad (1.8)$$

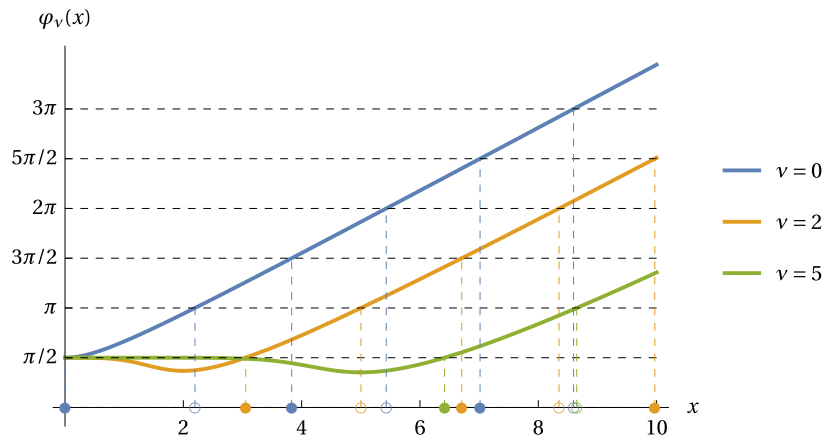


**Figure 5:** Plots of  $\varphi_\nu(x)$ . The filled colour-coded dots on the horizontal axis indicate the positions of zeros  $j'_{\nu,k}$  and the hollow dots the positions of zeros  $j_{\nu,k}$ . The phase functions are calculated using the method of [Hor7].

### §1.3. Our philosophy and some history

The main purpose of our paper is to present new uniform (in  $\nu$ ) two-sided bounds for the phase functions  $\theta_\nu(x)$  and  $\varphi_\nu(x)$  (Theorems 1.4 and 1.10), and, as a consequence, new bounds for the zeros of Bessel functions and their derivatives (Corollaries 1.6 and 1.12) valid, with minimal exceptions, for all  $\nu$  and  $k$ . Our bounds for the phase functions are expressed in terms of explicit elementary functions defined in §1.4 and §1.6, and the bounds for the zeros in terms of inverses of these functions. Additionally, due to the elementary nature of our bounds for phase functions, we derive simple bounds for the counting functions of zeros of Bessel functions and their derivatives (Corollaries 1.7 and 1.13), some of which have already been used to great effect in spectral-geometric problems, see [FLPS23] and [FLPS23a].

The common feature of our bounds and pre-existing bounds on zeros of Bessel functions and of their derivatives is that they are all based, in one form or another, on asymptotics of Bessel functions for large argument and/or order. We recall that there are, roughly speaking, three relevant asymptotic regimes, see [DLMF, §§10.17, 10.19–20]:

- (R<sub>i</sub>) the large-argument region, in which  $x$  approaches infinity and  $\nu$  is fixed (or at least bounded);
- (R<sub>ii</sub>) the transition region, in which  $\nu$  approaches infinity with  $x \sim \nu + a\nu^{1/3}$  for some  $a \in \mathbb{R}$ . In this region the Bessel functions exhibit Airy-type behaviour;
- (R<sub>iii</sub>) the Debye expansion region, in which  $\nu$  approaches infinity with  $x \sim c\nu$  for some  $c > 1$ .

Among the extensive historical literature on the topic we mention the work of Langer [L31] in the Debye region (R<sub>iii</sub>) and of Chester, Friedman, and Ursell [CFU57] in the transition region (R<sub>ii</sub>). For a modern perspective on the interplay between these regimes, see [S23].

The general previously used approach to bounding Bessel zeros is essentially based on using the asymptotics of Bessel zeros in either of the regimes (R<sub>i</sub>) or (R<sub>ii</sub>), and then applying a form of the Sturm comparison theorem. Some existing bounds for the zeros of Bessel functions obtained using the expansions in the large argument regime (R<sub>i</sub>) are due to Hethcote [He70] and Elbert–Laforgia [EL00], see also [GG00, GG07, N21]. The explicit expressions of these bounds, which we use for benchmarking purposes, are collected in §4. Note that the lower bounds for Bessel zeros obtained in this way are only available for very low values of  $\nu$ . Alternative bounds, based on the asymptotics of  $j_{\nu,k}$  in the transitional regime (R<sub>ii</sub>), are given by Qu and Wong [QW96], and are also presented in §4. There is significantly less information in the literature on uniform bounds for the

zeros  $J'_{\nu,k}$  of derivatives of Bessel functions: we failed to find any bounds derived from the asymptotics in the large argument regime ( $R_i$ ). The upper bound for  $J'_{\nu,k}$  derived from the asymptotics in the transitional regime ( $R_{ii}$ ) from [EL97], [Eoi, §1.7] is listed in §4.

Unlike the previous approaches, we choose to work directly with the phase functions  $\varphi_\nu(x)$  and  $\theta_\nu(x)$  instead, using their non-oscillatory character and their known asymptotics in the Debye expansion region ( $R_{iii}$ ). It has been known that these asymptotics give, in practice, good approximations of Bessel functions and their derivatives, and can be used for effective calculation of corresponding zeros with high precision, see [Hoi7] as well as various generalisations in the important series of papers by Bremer, Rokhlin, et al. [HBRV15, HBR15, BR16, B17, B19]. Using techniques of Olver, Horsley [Hoi7] has recently deduced asymptotics for the phase functions  $\theta_\nu(x)$  and  $\varphi_\nu(x)$  in the Debye region ( $R_{iii}$ ). An extremely helpful feature of this problem is that, as it turns out, the expansions in the Debye region also give effective expansions in the large-argument region, and only weaken when one proceeds deep into the transition region. Further, it turns out that truncating these expansions leads to lower and upper bounds for phase functions: the error terms are sign-definite for a broad range of values. We prove this using a consequence of the Sturm comparison theorem (Theorem 2.5) combined with the non-oscillatory nature of the phase functions. The more detailed comparison of our bounds with existing ones and their effectiveness will be addressed in §4.

The rest of the paper is organised as follows. In §§1.4–1.7, we define the necessary auxiliary functions, study their properties, and state our main results, illustrating them graphically. All the proofs, together with additional Sturm–Liouville theory required, are collected in §2. In §3, we extend our techniques to obtain the bounds on the zeros of derivatives of *ultraspherical* Bessel functions. As we have mentioned, §4 discusses the comparison of our results with older ones, based on numerical evidence collected in Appendix B. In order not to overload the main text, some complicated intermediate expressions are placed in Appendix A.

We remark that many of the proofs involve straightforward but rather cumbersome manipulations with explicit functions. Although we have verified them independently by hand, we have relied in some cases on simplifications using `Mathematica`. In the interest of transparency, the corresponding script, as well as its printout, containing *all* of the analytic and numerical calculations we performed, including plotting routines, is available for inspection and download at

<https://michaellevitin.net/bessels.html>.

#### §1.4. Definitions and properties of the auxiliary functions I

We start by defining the following auxiliary functions. Everywhere below  $x \geq \nu \geq 0$ .

We define

$$\tilde{\theta}_\nu(x) := \sqrt{x^2 - \nu^2} - \nu \arccos \frac{\nu}{x} - \frac{\pi}{4},$$

and note that

$$\tilde{\theta}_\nu(\nu) = -\frac{\pi}{4},$$

$$\tilde{\theta}_\nu(x) = x - \frac{\pi}{4}(2\nu + 1) + \frac{\nu^2}{2x} + O(x^{-3}) \quad \text{as } x \rightarrow +\infty. \tag{1.9}$$

We also note that

$$\tilde{\theta}'_\nu(x) = \frac{\sqrt{x^2 - \nu^2}}{x} > 0 \quad \text{for } x > \nu.$$

Therefore, the function  $\tilde{\theta}_\nu$  is strictly monotone increasing on the interval  $(\nu, +\infty)$ , and thus the inverse function

$$(\tilde{\theta}_\nu)^{-1} : \left[-\frac{\pi}{4}, +\infty\right) \rightarrow [\nu, +\infty)$$

is well-defined.

Further, we set

$$\underline{\theta}_\nu(x) := \tilde{\theta}_\nu(x) - \frac{3x^2 + 2\nu^2}{24(x^2 - \nu^2)^{3/2}} = \sqrt{x^2 - \nu^2} - \nu \arccos \frac{\nu}{x} - \frac{\pi}{4} - \frac{3x^2 + 2\nu^2}{24(x^2 - \nu^2)^{3/2}},$$

and note that

$$\begin{aligned} \underline{\theta}_\nu(x) &\rightarrow -\infty \quad \text{as } x \rightarrow \nu^+, \\ \underline{\theta}_\nu(x) &= x - \frac{\pi}{4}(2\nu + 1) + \frac{4\nu^2 - 1}{8x} + \frac{\nu^2(2\nu^2 - 13)}{48x^3} + O(x^{-5}) \quad \text{as } x \rightarrow +\infty. \end{aligned} \quad (1.10)$$

We also have

$$\underline{\theta}'_\nu(x) = \frac{8x^6 + (1 - 24\nu^2)x^4 + 4(6\nu^4 + \nu^2)x^2 - 8\nu^6}{8x(x^2 - \nu^2)^{5/2}},$$

and therefore

$$\underline{\theta}'_\nu\left(\sqrt{\nu^2 + \chi}\right) = \frac{8\chi^3 + \chi^2 + 6\chi\nu^2 + 5\nu^4}{8\chi^{5/2}\sqrt{\nu^2 + \chi}} > 0 \quad \text{for } \chi > 0.$$

Hence the function  $\underline{\theta}_\nu$  is strictly monotone increasing on the interval  $(\nu, +\infty)$ , and the inverse function

$$(\underline{\theta}_\nu)^{-1} : \mathbb{R} \rightarrow (\nu, +\infty)$$

is well-defined.

*Remark 1.3.* We should explain the origin of the functions  $\tilde{\theta}_\nu(x)$  and  $\underline{\theta}_\nu(x)$ : they represent, correspondingly, the two- and three-term asymptotic expansions of  $\theta_\nu(x)$  in the Debye regime (R<sub>iii</sub>), see [Hor7, formula (34)], which are obtained using the algorithm of [O74]. ◀

### §1.5. Main results I: bounding the phase and zeros of Bessel functions

Set, for  $x > \nu \geq 0$ ,

$$\underline{\underline{\theta}}_\nu(x) := \max\left\{\underline{\theta}_\nu(x), -\frac{\pi}{2}\right\}.$$

We have

**Theorem 1.4.** *For every  $\nu \geq 0$  and every  $x > \nu$ ,*

$$\underline{\underline{\theta}}_\nu(x) < \theta_\nu(x) < \tilde{\theta}_\nu(x). \quad (1.11)$$

*Remark 1.5.* The upper bound in Theorem 1.4 has been already proved, using different techniques, in [S23] and [FLPS23]. ◀

Recalling (1.2) and (1.3), Theorem 1.4 immediately implies

**Corollary 1.6.** *For every  $\nu \geq 0$ , we have the following bounds.*

(i) *For every  $k \in \mathbb{N}$ ,*

$$\underline{\underline{j}}_{\nu,k} := (\underline{\underline{\theta}}_\nu)^{-1}\left(\pi\left(k - \frac{1}{2}\right)\right) < j_{\nu,k} < (\underline{\theta}_\nu)^{-1}\left(\pi\left(k - \frac{1}{2}\right)\right) =: \tilde{j}_{\nu,k}.$$

(ii) *For every  $k \in \mathbb{N}$ ,*

$$\underline{\underline{y}}_{\nu,k} := (\underline{\underline{\theta}}_\nu)^{-1}(\pi(k-1)) < y_{\nu,k} < (\underline{\theta}_\nu)^{-1}(\pi(k-1)) =: \tilde{y}_{\nu,k}.$$

(iii) More generally, for all  $\tau \in (0, 1]$  and all  $k \geq 2$ , we have

$$\mathcal{L}_{v,\tau,k} := (\tilde{\theta}_v)^{-1} \left( \pi \left( \tau + k - \frac{3}{2} \right) \right) < c_{v,\tau,k} < (\underline{\theta}_v)^{-1} \left( \pi \left( \tau + k - \frac{3}{2} \right) \right) =: \tilde{c}_{v,\tau,k}.$$

For  $k = 1$ , the upper bound  $c_{v,\tau,1} < \tilde{c}_{v,\tau,1}$  is also valid for all  $\tau \in (0, 1]$ , and the lower bound  $\mathcal{L}_{v,\tau,1} < c_{v,\tau,1}$  is valid for  $\tau \in (\frac{1}{4}, 1]$ .

In part (iii), the restriction on the range of  $\tau$  for which the lower bound holds with  $k = 1$  is due to the necessary condition  $\pi \left( \tau + \frac{1}{2} \right) > -\frac{\pi}{4}$  for applying the inverse function.

For an illustration of the results in Theorem 1.4 and Corollary 1.6, see Figure 6.

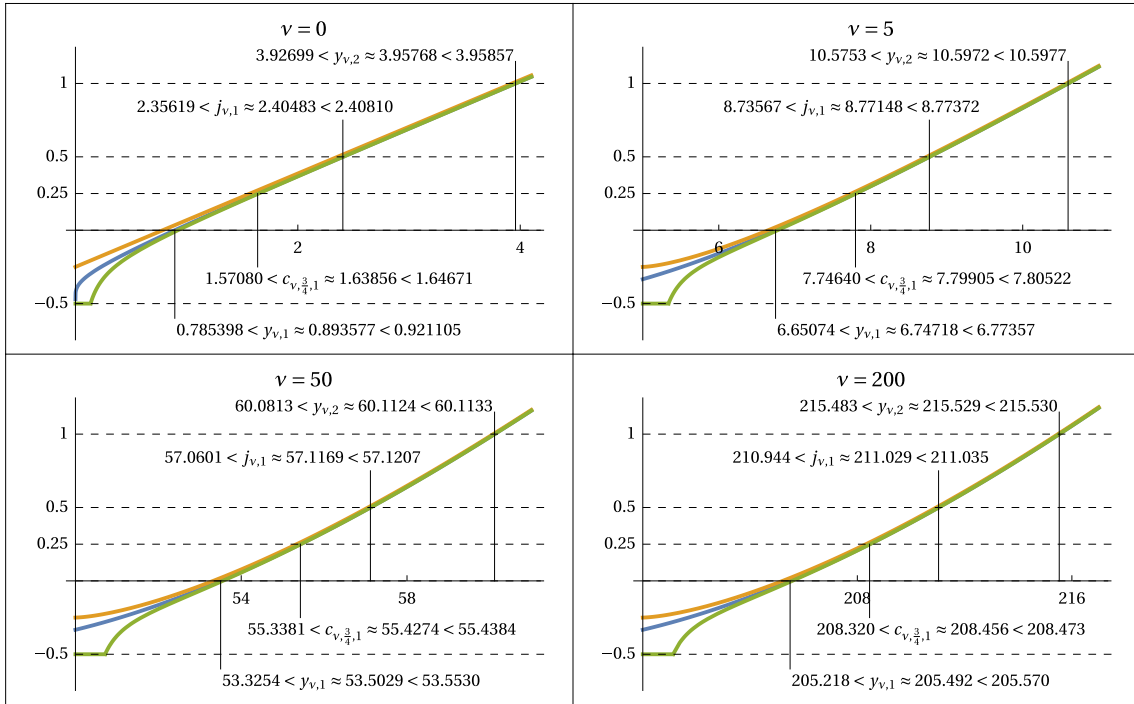


**Figure 6:** All plots show the scaled Bessel phase function  $\frac{1}{\pi}\theta_\nu(x)$  (blue), and its scaled bounds  $\frac{1}{\pi}\tilde{\theta}_\nu(x)$  (orange) and  $\frac{1}{\pi}\underline{\theta}_\nu(x)$  (green). The zeros  $c_{\nu, \frac{3}{4}, 1}$  are the first positive zeros of  $\mathcal{C}_{\nu, \frac{3}{4}}(x)$ , which up to a constant factor coincides with  $J_\nu(x) - Y_\nu(x)$ .

We also immediately deduce the bounds for the counting function (1.4) of Bessel zeros.

**Corollary 1.7.** For any  $\lambda > \nu \geq 0$ ,

$$\left\lfloor \frac{1}{\pi} \underline{\theta}_\nu(\lambda) + \frac{1}{2} \right\rfloor \leq \mathcal{N}_{J_\nu}(\lambda) \leq \left\lfloor \frac{1}{\pi} \tilde{\theta}_\nu(\lambda) + \frac{1}{2} \right\rfloor,$$

where  $\lfloor \cdot \rfloor$  denotes the integer part.

### §1.6. Definitions and properties of the auxiliary functions II

We define, for  $x > \nu \geq 0$ , the functions

$$\underline{\varphi}_\nu(x) := \tilde{\theta}_\nu(x) + \frac{\pi}{2} = \sqrt{x^2 - \nu^2} - \nu \arccos \frac{\nu}{x} + \frac{\pi}{4}, \quad (1.12)$$

and

$$\tilde{\varphi}_\nu(x) := \underline{\varphi}_\nu(x) + \frac{9x^2 - 2\nu^2}{24(x^2 - \nu^2)^{3/2}} = \sqrt{x^2 - \nu^2} - \nu \arccos \frac{\nu}{x} + \frac{\pi}{4} + \frac{9x^2 - 2\nu^2}{24(x^2 - \nu^2)^{3/2}}.$$

As in §1.4, we have

$$\begin{aligned} \underline{\varphi}_\nu(\nu) &= \frac{\pi}{4}, \\ \underline{\varphi}_\nu(x) &= x - \frac{\pi}{4}(2\nu - 1) + \frac{\nu^2}{2x} + O(x^{-3}) \quad \text{as } x \rightarrow +\infty. \end{aligned} \quad (1.13)$$

Also,

$$\underline{\varphi}'_\nu(x) = \tilde{\theta}'_\nu(x) > 0 \quad \text{for all } x > \nu \geq 0,$$

and the inverse function

$$\left(\underline{\varphi}_\nu\right)^{-1} : \left[\frac{\pi}{4}, +\infty\right) \rightarrow [\nu, +\infty)$$

is well-defined. Moreover,

$$\left(\underline{\varphi}_\nu\right)^{-1}(z) = \left(\tilde{\theta}_\nu\right)^{-1}\left(z - \frac{\pi}{2}\right).$$

The behaviour of the function  $\tilde{\varphi}_\nu(x)$  is more complicated. We have

$$\tilde{\varphi}_\nu(x) \rightarrow +\infty \quad \text{as } x \rightarrow \nu^+,$$

and

$$\tilde{\varphi}_\nu(x) = x - \frac{\pi}{4}(2\nu - 1) + \frac{4\nu^2 + 3}{8x} + \frac{\nu^2(2\nu^2 + 23)}{48x^3} + O(x^{-5}) \quad \text{as } x \rightarrow +\infty. \quad (1.14)$$

Further,

$$\tilde{\varphi}'_\nu(x) = \frac{p_\nu(x)}{8x(x^2 - \nu^2)^{5/2}},$$

where

$$p_\nu(x) := 8x^6 - 3(8\nu^2 + 1)x^4 + 4\nu^2(6\nu^2 - 1)x^2 - 8\nu^6 \quad (1.15)$$

is not sign-definite for  $x \in [\nu, +\infty)$ . Namely, we will prove

**Lemma 1.8.** *For any  $\nu \geq 0$ , we have  $\tilde{\varphi}'_\nu(x) > 0$  for  $x \in (x_\nu^*, +\infty)$ , where  $x_\nu^*$  is the only root in  $(\nu, +\infty)$  of (1.15). The quantity*

$$z_\nu^* := \tilde{\varphi}_\nu(x_\nu^*)$$

*is positive and monotone decreasing in  $\nu$  for all  $\nu \geq 0$ .*

We present the graph of  $\frac{1}{\pi}z_\nu^*$  as a function of  $\nu$  in Figure 7. Note that  $x_0^* = \sqrt{\frac{3}{8}}$  and  $z_0^* = \frac{\pi}{4} + \sqrt{\frac{3}{2}}$ . It may be also shown that

$$x_\nu^* = \nu + \frac{\sqrt[3]{7\nu}}{4} + O(\nu^{-1/3}), \quad z_\nu^* = \frac{\pi}{4} + \sqrt{\frac{7}{18}} + O(\nu^{-2/3}) \quad \text{as } \nu \rightarrow +\infty.$$

Lemma 1.8 now ensures that the inverse function

$$\left(\underline{\varphi}_\nu\right)^{-1} : [z_\nu^*, +\infty) \rightarrow [x_\nu^*, +\infty)$$

is well-defined.

*Remark 1.9.* Similarly to Remark 1.3, the functions  $\underline{\varphi}_\nu(x)$  and  $\tilde{\varphi}_\nu(x)$  represent, correspondingly, the two- and three-term asymptotic expansions of  $\varphi_\nu(x)$  in the Debye regime (R<sub>iii</sub>), see [Hor7, formula (46)]. ◀

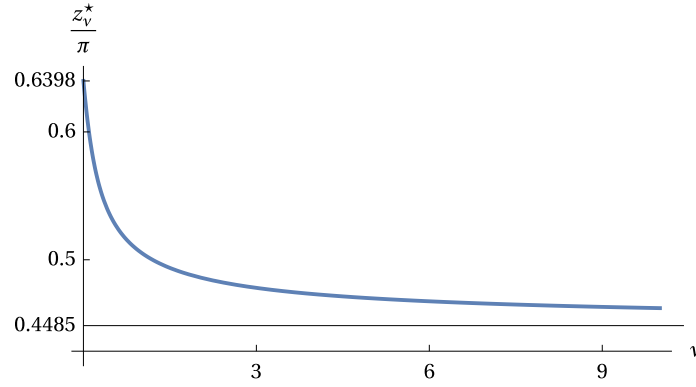


**Figure 7:** The plot of  $\frac{1}{\pi} z_v^*$  against  $\nu$ , with the horizontal asymptote positioned at an approximate value of  $\frac{1}{4} + \frac{1}{\pi} \sqrt{\frac{7}{18}}$ .

### §1.7. Main results II: bounding the phase and zeros of derivatives of Bessel functions

Set, for  $x > \nu \geq 0$ ,

$$\tilde{\varphi}_\nu(x) := \begin{cases} z_\nu^* & \text{if } x < x_\nu^*, \\ \tilde{\varphi}_\nu(x) & \text{if } x \geq x_\nu^*. \end{cases}$$

**Theorem 1.10.** For every  $\nu \geq 0$  and every  $x > \nu$ , we have

$$\varphi_\nu(x) < \varphi_\nu(x) < \tilde{\varphi}_\nu(x). \quad (1.16)$$

*Remark 1.11.* The lower bound in Theorem 1.10 has been already proved, using different techniques, in [FLPS23]. ◀

Recalling (1.6) and (1.7), Theorem 1.10 immediately implies

**Corollary 1.12.** For every  $\nu \geq 0$ , we have the following bounds.

(i) For every  $k \in \{2, 3, \dots\}$ ,

$$\underline{j}'_{\nu,k} := (\tilde{\varphi}_\nu)^{-1} \left( \pi \left( k - \frac{1}{2} \right) \right) < j'_{\nu,k} < (\varphi_\nu)^{-1} \left( \pi \left( k - \frac{1}{2} \right) \right) =: \tilde{j}'_{\nu,k}.$$

For  $k = 1$ , the upper bound  $j'_{\nu,1} < \tilde{j}'_{\nu,1}$  is also valid for all  $\nu \geq 0$ , and the lower bound  $\underline{j}'_{\nu,1} < j'_{\nu,1}$  is valid whenever

$$z_\nu^* \leq \frac{\pi}{2},$$

that is, roughly, for  $\nu \gtrsim 1.19876$ .

(ii) For every  $k \in \mathbb{N}$ ,

$$\underline{y}'_{\nu,k} := (\tilde{\varphi}_\nu)^{-1}(\pi k) < y'_{\nu,k} < (\varphi_\nu)^{-1}(\pi k) =: \tilde{y}'_{\nu,k}.$$

(iii) More generally, for all  $\tau \in [0, 1)$  and all  $k \geq 2$ , we have

$$\underline{c}'_{\nu,\tau,k} := (\tilde{\varphi}_\nu)^{-1} \left( \pi \left( \tau + k - \frac{1}{2} \right) \right) < c'_{\nu,\tau,k} < (\varphi_\nu)^{-1} \left( \pi \left( \tau + k - \frac{1}{2} \right) \right) =: \tilde{c}'_{\nu,\tau,k}.$$

For  $k = 1$ , the upper bound  $c'_{\nu,\tau,1} < \tilde{c}'_{\nu,\tau,1}$  is also valid for all  $\tau \in [0, 1)$ . The lower bound  $\underline{c}'_{\nu,\tau,1} < c'_{\nu,\tau,1}$  is valid for  $\nu$  such that

$$z_\nu^* \leq \pi \left( \tau + \frac{1}{2} \right);$$

in particular, if  $\tau \geq \frac{1}{\pi} z_0^* - \frac{1}{2} = \frac{1}{\pi} \sqrt{\frac{3}{2}} - \frac{1}{4} \approx 0.139848$ , then it is valid for all  $\nu \geq 0$ , see Figure 8.

In parts (i) and (iii), the restriction on the range of  $\nu$  and  $\tau$  for which the lower bound holds with  $k = 1$  is due to the fact that the argument of the inverse function  $(\tilde{\varphi}_\nu)^{-1}$  should exceed  $z_\nu^*$ .

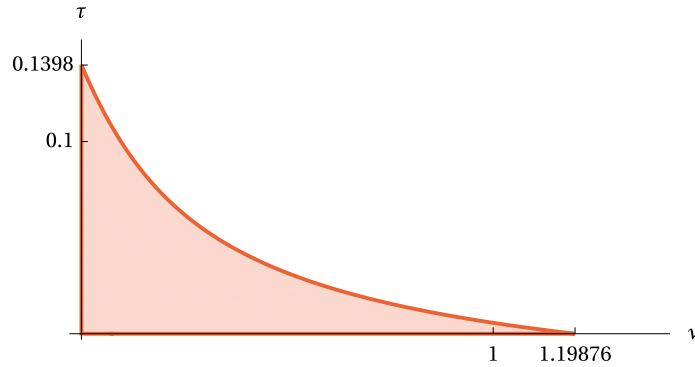


**Figure 8:** The region of the  $(\nu, \tau)$ -plane in which the lower bound  $\mathcal{L}'_{\nu, \tau, 1} < c'_{\nu, \tau, 1}$  for the first zero is *not applicable*.

For an illustration of the results in Theorem 1.10 and Corollary 1.12, see Figure 9.

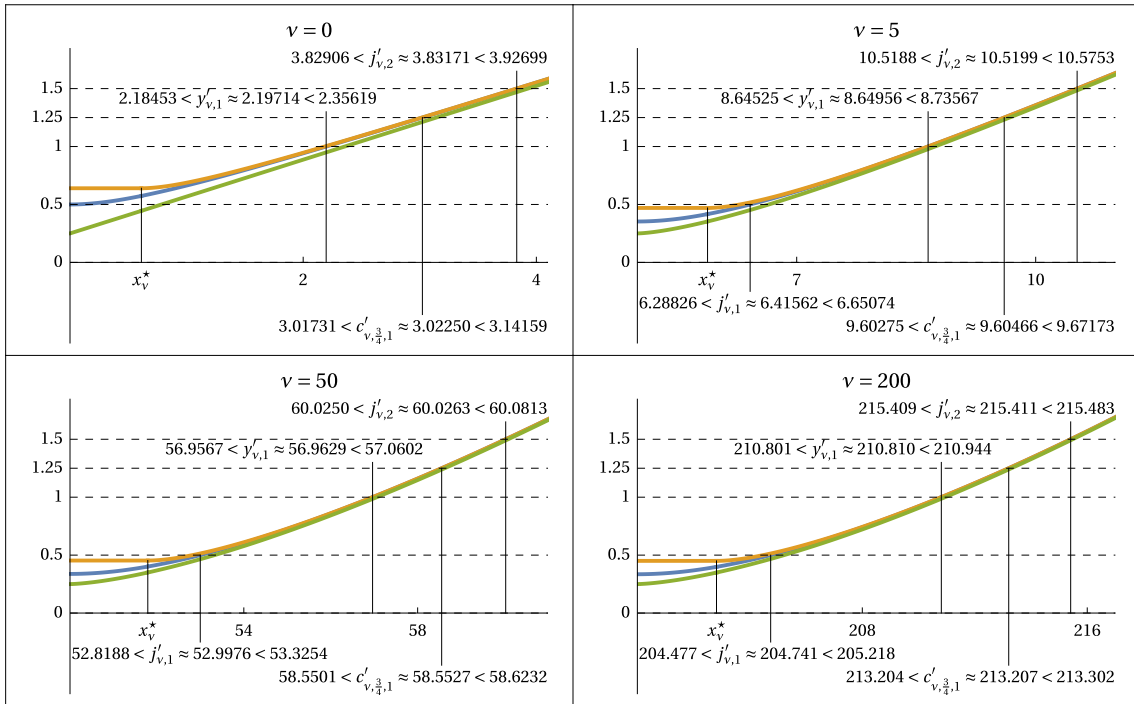


**Figure 9:** All plots show the scaled Bessel derivative phase function  $\frac{1}{\pi} \varphi_\nu(x)$  (blue), and its scaled bounds  $\frac{1}{\pi} \tilde{\varphi}_\nu(x)$  (orange) and  $\varphi_\nu(x)$  (green). The zeros  $c'_{\nu, \frac{3}{4}, 1}$  are the first zeros above  $j'_{\nu, 1}$  of  $\mathcal{C}'_{\nu, \frac{3}{4}}(x)$ , which up to a constant factor coincides with  $J'_\nu(x) - Y'_\nu(x)$ .

We also immediately deduce the bounds for the counting function (1.8) of zeros of Bessel derivatives.

**Corollary 1.13.** For any  $\lambda > \nu \geq 0$ ,

$$\left\lfloor \frac{1}{\pi} \varphi_\nu(\lambda) + \frac{1}{2} \right\rfloor \leq \mathcal{N}'_\nu(\lambda) \leq \left\lfloor \frac{1}{\pi} \tilde{\varphi}_\nu(\lambda) + \frac{1}{2} \right\rfloor.$$

## §2. Proofs

### §2.1. Liouville's transformation and phase functions

Consider a real-valued function  $f \in C^3(a, +\infty)$ ,  $a \in \mathbb{R}$ , with  $f'(x) > 0$  for  $x > a$ . For  $t \in \mathbb{R}$ , we define the functions

$$\mathcal{F}_{f,t}(x) := \frac{\cos(f(x) - \pi t)}{\sqrt{f'(x)}}$$

and

$$\mathcal{V}_f(x) := (f'(x))^2 + \frac{1}{2} \frac{f'''(x)}{f'(x)} - \frac{3}{4} \left( \frac{f''(x)}{f'(x)} \right)^2. \quad (2.1)$$

The following simple result is verified by a direct substitution, cf. [ELoo, Lemma 1].

**Lemma 2.1.** *Under the above conditions, the function  $\mathcal{F}_{f,t}(x)$  satisfies on  $(a, +\infty)$  the Schrödinger equation*

$$\mathcal{F}_{f,t}''(x) + \mathcal{V}_f(x) \mathcal{F}_{f,t}(x) = 0. \quad (2.2)$$

*Remark 2.2.* The relation (2.1) is called *Liouville's transformation* in [Hoi7] and *Kummer's equation* in [HBRV15, §1]. ◀

Let now  $\mathcal{A}_1(x)$  and  $\mathcal{A}_2(x)$  be two real linearly independent solutions of a Schrödinger equation

$$\mathcal{A}''(x) + \mathcal{P}(x) \mathcal{A}(x) = 0 \quad (2.3)$$

on  $(a, +\infty)$ , with a real-valued potential  $\mathcal{P} \in C(a, +\infty)$ . We define the modulus function  $\mathcal{M}(x) = \mathcal{M}_{\mathcal{A}_1, \mathcal{A}_2}(x)$  and the phase function  $\Psi(x) = \Psi_{\mathcal{A}_1, \mathcal{A}_2}(x)$  for these solutions as

$$\mathcal{M}(x) := \sqrt{(\mathcal{A}_1(x))^2 + (\mathcal{A}_2(x))^2}, \quad \mathcal{A}_1(x) + i\mathcal{A}_2(x) = \mathcal{M}(x) \exp(i\Psi(x)),$$

where we choose a continuous branch of  $\Psi(x) = \text{Arctan} \frac{\mathcal{A}_2(x)}{\mathcal{A}_1(x)}$  specified by the chosen value of

$$\lim_{x \rightarrow a^+} \Psi(x).$$

**Lemma 2.3.** *We have*

$$\Psi'(x) = \frac{\mathcal{W}\{\mathcal{A}_1(x), \mathcal{A}_2(x)\}}{\mathcal{M}(x)^2},$$

where  $\mathcal{W}\{\cdot, \cdot\}$  is the Wronskian of the two solutions, cf. [HBRV15, §1].

*Assume additionally that  $\Psi'(x) > 0$  for  $x \in (a, +\infty)$ . Then for any  $t \in \mathbb{R}$ , the function*

$$\mathcal{A}(x) := \mathcal{F}_{\Psi,t}(x)$$

*also satisfies (2.3), and therefore*

$$\mathcal{V}_{\Psi}(x) = \mathcal{P}(x).$$

*Proof.* The first statement is verified by direct differentiation:

$$\Psi'(x) = \frac{d}{dx} \arctan \frac{\mathcal{A}_2(x)}{\mathcal{A}_1(x)} = \frac{\mathcal{A}_1(x) \mathcal{A}_2'(x) - \mathcal{A}_2(x) \mathcal{A}_1'(x)}{(\mathcal{A}_1(x))^2 + (\mathcal{A}_2(x))^2}.$$

Since

$$\mathcal{F}_{\Psi,t}(x) = \frac{\cos(\pi t) \mathcal{A}_1(x) + \sin(\pi t) \mathcal{A}_2(x)}{\sqrt{\mathcal{W}}},$$

where  $\mathcal{W} = \mathcal{W}\{\mathcal{A}_1(x), \mathcal{A}_2(x)\}$  is a constant which we assumed to be positive, the second statement also follows immediately once we have taken into account that  $\mathcal{A}_1(x)$  and  $\mathcal{A}_2(x)$  both satisfy (2.3). ◻

Lemma 2.3 implies

**Lemma 2.4.** *For the Bessel phase function  $\theta_\nu(x)$ , we have the Schrödinger equation (2.2), namely,*

$$\mathcal{F}_{\theta_\nu, t}''(x) + \mathcal{V}_{\theta_\nu}(x)\mathcal{F}_{\theta_\nu, t}(x) = 0$$

valid in the interval  $(0, +\infty)$  for all  $\nu \geq 0$  and  $t \in \mathbb{R}$ , with

$$\mathcal{V}_{\theta_\nu}(x) = 1 - \frac{\nu^2 - 1/4}{x^2}. \quad (2.4)$$

Similarly, for the Bessel derivative phase function  $\varphi_\nu(x)$ , we also have the Schrödinger equation (2.2), namely,

$$\mathcal{F}_{\varphi_\nu, t}''(x) + \mathcal{V}_{\varphi_\nu}(x)\mathcal{F}_{\varphi_\nu, t}(x) = 0$$

valid in the interval  $(\nu, +\infty)$  for all  $\nu \geq 0$  and  $t \in \mathbb{R}$ , with

$$\mathcal{V}_{\varphi_\nu}(x) = 1 - \frac{\nu^2 - \frac{1}{4}}{x^2} - \frac{2\nu^2 + x^2}{(x^2 - \nu^2)^2}. \quad (2.5)$$

*Proof.* We note that for all cylindrical functions  $\mathcal{C}_{\nu, \tau}(x)$ , and in particular for  $J_\nu(x)$  and  $Y_\nu(x)$ , we have the Schrödinger equation

$$(\sqrt{x}\mathcal{C}_{\nu, \tau}(x))'' + \left(1 - \frac{\nu^2 - 1/4}{x^2}\right)(\sqrt{x}\mathcal{C}_{\nu, \tau}(x)) = 0,$$

see [DLMF, (10.13.1)]; it can be easily checked directly. By Lemma 2.3, since  $\theta_\nu(x) = \Psi_{\sqrt{x}J_\nu, \sqrt{x}Y_\nu}(x)$  has a positive derivative on  $(\nu, +\infty)$ , we conclude that  $\mathcal{F}_{\varphi_\nu, t}$  satisfies the Schrödinger equation with the same potential, thus proving (2.4). We note that (2.4) can be found in [DLMF, (10.18.16)].

In the same manner, we have for  $\mathcal{C}'_{\nu, \tau}(x)$ , and in particular for  $J'_\nu(x)$  and  $Y'_\nu(x)$ ,

$$\left(\frac{x^{3/2}}{\sqrt{x^2 - \nu^2}} \mathcal{C}'_{\nu, \tau}(x)\right)'' + \left(1 - \frac{\nu^2 - \frac{1}{4}}{x^2} - \frac{2\nu^2 + x^2}{(x^2 - \nu^2)^2}\right)\left(\frac{x^{3/2}}{\sqrt{x^2 - \nu^2}} \mathcal{C}'_{\nu, \tau}(x)\right) = 0,$$

which is straightforward to verify directly or deduce from [DLMF, (10.13.7)], and the result follows from the observation that  $\varphi_\nu(x) = \Psi_{\frac{x^{3/2}}{\sqrt{x^2 - \nu^2}} J'_\nu, \frac{x^{3/2}}{\sqrt{x^2 - \nu^2}} Y'_\nu}(x)$  has a positive derivative on  $(\nu, +\infty)$ .  $\square$

## §2.2. A consequence of the Sturm comparison theorem

We state the following result which follows from the Sturm comparison theorem, and which will be used for comparing phase functions and their bounds. This is different from a common method of comparing zeros, cf. [He70] and [ELoo].

**Theorem 2.5.** *Consider, for  $a \in \mathbb{R}$ , two functions  $g, h \in C^3(a, +\infty)$  with positive derivatives and satisfying the following conditions:*

- (C<sub>1</sub>)  $\lim_{x \rightarrow +\infty} g(x) = \lim_{x \rightarrow +\infty} h(x) = +\infty$ ;
- (C<sub>2</sub>)  $\mathcal{V}_g(x) > \mathcal{V}_h(x)$  for all  $x \in (a, +\infty)$ ;
- (C<sub>3</sub>) there exists  $b \geq a$  such that  $g(x) < h(x)$  for all  $x > b$ .

Then in fact  $g(x) < h(x)$  for all  $x > a$ .

*Remark 2.6.* Our typical use of Theorem 2.5 can be illustrated by the following generic example.

Suppose that  $g(x)$  is a phase function  $\Psi_{\mathcal{A}_1, \mathcal{A}_2}(x)$  of two linearly independent solutions of the Schrödinger equation (2.3) with a given potential  $\mathcal{P}(x)$ , and  $h(x)$  is some conjectured upper bound for  $g(x)$ . Assuming that both  $g(x)$  and  $h(x)$  have positive derivatives, we can use Lemma 2.3 to deduce that  $\mathcal{V}_g(x) = \mathcal{P}(x)$ , and therefore verification of  $(C_2)$  reduces to an explicit calculation.

In practice, we usually replace condition  $(C_3)$  by a stronger condition

$(C'_3)$  for some  $s \in \mathbb{R}$ , there exists the limit  $\lim_{x \rightarrow +\infty} x^s (h(x) - g(x))$ , and it is positive.

This condition is easier to verify if the asymptotics of the phase function as  $x \rightarrow +\infty$  is known. It is clear that  $(C'_3)$  implies  $(C_3)$ . ◀

*Proof of Theorem 2.5.* Suppose that the conclusion is wrong. Then there exists  $x_0 > a$  for which  $g(x_0) \geq h(x_0)$ . Let  $h_0 := h(x_0)$ ,  $t_0 := \frac{1}{\pi} h_0 - \frac{1}{2}$ , and consider the following two functions,

$$G(x) := \mathcal{F}_{g, t_0}(x) = \frac{\sin(g(x) - h_0)}{\sqrt{g'(x)}}, \quad H(x) := \mathcal{F}_{h, t_0}(x) = \frac{\sin(h(x) - h_0)}{\sqrt{h'(x)}}.$$

Our assumptions imply that these function are both in  $C^2(a, \infty)$ , and, by Lemma 2.1, satisfy the differential equations

$$G''(x) + \mathcal{V}_g(x)G(x) = 0, \quad H''(x) + \mathcal{V}_h(x)H(x) = 0$$

in that interval.

Due to condition  $(C_1)$ ,  $H(x)$  has infinitely many zeros  $\eta_k \in [x_0, \infty)$ , one each time  $h(\eta_k) - h_0 = \pi k$ , for some sequence of consecutive  $k \in \mathbb{Z}$ . Note that  $\eta_0 = x_0$ , so that this sequence starts with  $k = 0$ . Similarly,  $G(x)$  has a zero  $\gamma_k \in [x_0, \infty)$  each time  $g(\gamma_k) - h_0 = \pi k$  for another sequence of consecutive  $k \in \mathbb{Z}$ . Equivalently,

$$\gamma_k = g^{-1}(\pi k + h_0), \quad \eta_k = h^{-1}(\pi k + h_0). \quad (2.6)$$

Observe that by our contradiction assumption,  $g(x_0) - h_0 \geq 0$ , or  $\gamma_0 = g^{-1}(h_0) \leq x_0$ , and so the first zero of  $G(x)$  in  $(x_0, \infty)$  is  $\gamma_m$  for some  $m > 0$ . By condition  $(C_2)$  and the Sturm comparison theorem, there exists at least one zero of  $G(x)$  strictly between each pair of zeros of  $H(x)$  on  $(x_0, \infty)$ . So,  $G(x)$  has a zero in  $(\eta_0, \eta_1)$ , and therefore we must have

$$\gamma_m < \eta_1 \leq \eta_m.$$

Similarly, there must be a zero of  $G(x)$  in  $(\eta_m, \eta_{m+1})$ , and therefore  $\gamma_{m+1} < \eta_{m+1}$ . By induction,  $\gamma_k < \eta_k$  for all  $k \geq m$ . However, by (2.6) and condition  $(C_3)$ , we must have  $\gamma_k > \eta_k$  for sufficiently large  $k$ . This contradiction completes the proof. ◻

### §2.3. Proof of Theorem 1.4

We start with the upper bound. Applying Lemma 2.1 to  $f := \tilde{\theta}_v$  (which is defined and has a positive derivative on  $(v, +\infty)$ ) with  $t = 0$ , we deduce that on this interval the function  $\mathcal{F}_{\tilde{\theta}_v, 0}$  satisfies the Schrödinger equation

$$\mathcal{F}_{\tilde{\theta}_v, 0}''(x) + \mathcal{V}_{\tilde{\theta}_v}(x)\mathcal{F}_{\tilde{\theta}_v, 0}(x) = 0,$$

with the potential

$$\mathcal{V}_{\tilde{\theta}_v}(x) = \frac{4x^6 - 12v^2x^4 + 6v^2(2v^2 - 1)x^2 - v^4(4v^2 - 1)}{4x^2(x^2 - v^2)^2}. \quad (2.7)$$

We want to apply Theorem 2.5 with

$$g(x) = \theta_v(x), \quad h(x) = \tilde{\theta}_v(x), \quad a = v.$$

Condition (C<sub>1</sub>) of Theorem 2.5 is obviously true. Verifying condition (C<sub>2</sub>) is straightforward: we have, by (2.7) and (2.4),

$$\mathcal{V}_{\theta_v}(x) - \mathcal{V}_{\tilde{\theta}_v}(x) = \frac{x^2 + 4v^2}{4(x^2 - v^2)^2} > 0 \quad \text{for all } x > v.$$

According to Remark 2.6, it remains to check condition (C'<sub>3</sub>). The comparison of the asymptotics (1.1) and (1.9) yields

$$\tilde{\theta}_v(x) - \theta_v(x) = \frac{1}{8x} + O(x^{-3}) \quad \text{as } x \rightarrow +\infty,$$

and therefore (C'<sub>3</sub>) holds in this case with  $s = 1$ . Thus all conditions of Theorem 2.5 are fulfilled, which proves the upper bound in (1.11).

Instead of proving the lower bound in (1.11), we first establish a weaker bound

$$\underline{\theta}_v(x) < \theta_v(x). \quad (2.8)$$

In order to prove (2.8) we act in the same manner as above, this time applying Theorem 2.5 with

$$g(x) = \underline{\theta}_v(x), \quad h(x) = \theta_v(x), \quad a = v.$$

The expression for  $\mathcal{V}_{\underline{\theta}_v}(x)$  is given in Appendix A.

Condition (C<sub>1</sub>) of Theorem 2.5 is obviously true, and verifying condition (C<sub>2</sub>) requires the change of variable  $x = \sqrt{v^2 + \chi}$  with  $\chi > 0$ , which gives, by (2.4) and (A.1)–(A.3),

$$\begin{aligned} & 64\chi^5 (8\chi^3 + \chi^2 + 6v^2\chi + 5v^4)^2 \left( \mathcal{V}_{\underline{\theta}_v}(\sqrt{v^2 + \chi}) - \mathcal{V}_{\theta_v}(\sqrt{v^2 + \chi}) \right) = \\ & 1600\chi^9 + (33984v^2 + 16)\chi^8 + (99008v^4 + 784v^2 + 1)\chi^7 \\ & + (70720v^4 + 1696v^2 + 23)v^2\chi^6 + 3(1376v^2 + 71)v^4\chi^5 + (5200v^2 + 1011)v^6\chi^4 \\ & + 5(400v^2 + 519)v^8\chi^3 + 3525v^{10}\chi^2 + 2375v^{12}\chi + 625v^{14}. \end{aligned}$$

The right-hand side and the factor in the left-hand side are obviously positive for all  $\chi > 0$ , and thus  $\mathcal{V}_{\underline{\theta}_v}(x) > \mathcal{V}_{\theta_v}(x)$  for all  $x > v$ .

The validity of condition (C'<sub>3</sub>) follows from comparing (1.1) and (1.10), which gives

$$\theta_v(x) - \underline{\theta}_v(x) = \frac{25}{384x^3} + O(x^{-4}) \quad \text{as } x \rightarrow +\infty,$$

which implies (C'<sub>3</sub>) with  $s = 3$ . This shows that Theorem 2.5 is applicable and proves (2.8). The lower bound in (1.11) now follows as we know a priori that  $\theta_v(x) > -\frac{\pi}{2}$  for all  $x > v \geq 0$ .

#### §2.4. Proof of Lemma 1.8

The only two non-trivial aspects are that the root  $x_v^*$  of the sextic polynomial (1.15) is greater than  $v$ , and that  $z_v^*$  is monotone decreasing in  $v$ .

To address the former, the substitution  $x = \sqrt{v^2 + \xi}$ ,  $\xi \geq 0$ , turns (1.15) into

$$p_v(\sqrt{v^2 + \xi}) = 8\xi^3 - 3\xi^2 - 10v^2\xi - 7v^4.$$

It is then elementary to check that  $p_v(v) \leq 0$ ,  $p_v(\sqrt{v^2 + \xi})$  is negative near  $\xi = 0^+$ , positive as  $\xi \rightarrow +\infty$ , and  $\frac{dp_v(\sqrt{v^2 + \xi})}{d\xi}$  vanishes at the only positive point  $\xi = \frac{1}{8} + \frac{\sqrt{80v^2 + 3}}{8\sqrt{3}}$ , which completes the proof.

To address the latter aspect, suppose for contradiction that  $\frac{dz_v^*}{dv}$  vanishes for some  $v = \mu > 0$ . We have

$$0 = \left. \frac{dz_v^*}{dv} \right|_{v=\mu} = \left. \frac{d\tilde{\varphi}_v(x_v^*)}{dv} \right|_{v=\mu} = \left. \frac{\partial \tilde{\varphi}_v(x)}{\partial v} \right|_{(v,x)=(\mu,x_\mu^*)} + \tilde{\varphi}'_\mu(x_\mu^*) \left. \frac{dx_v^*}{dv} \right|_{v=\mu}. \quad (2.9)$$

The last term in the right-hand side (in which  $'$  denotes, as usual, the derivative with respect to the argument), vanishes by the definition of  $x_v^*$ , and the equation reduces, after explicit evaluation of  $\frac{\partial \tilde{\varphi}_v(x)}{\partial v}$  and the substitution

$$x_\mu^* = \kappa \mu \quad \text{with } \kappa > 1, \quad (2.10)$$

to

$$\mu^2 = \frac{23\kappa^2 - 2}{24(\kappa^2 - 1)^{5/2} \operatorname{arcsec} \kappa}. \quad (2.11)$$

We now recall that by (1.15) we still require

$$p_\mu(x_\mu^*) = 0;$$

substituting (2.10) and (2.11) into this gives, after some simplifications and using  $\kappa > 1$ , the equation

$$\frac{23\kappa^4 - 25\kappa^2 + 2}{3\kappa^2 \sqrt{\kappa^2 - 1} (3\kappa^2 + 4)} - \operatorname{arcsec} \kappa = 0. \quad (2.12)$$

Denote the left-hand side of (2.12) by  $K(\kappa)$ . Then  $\lim_{\kappa \rightarrow 1^+} K(\kappa) = 0$  and

$$K'(\kappa) = -\frac{16(\kappa^2 - 1)^{3/2} (6\kappa^2 + 1)}{3\kappa^3 (3\kappa^2 + 4)^2}$$

is strictly negative for  $\kappa > 1$ . Therefore (2.12) cannot have any solutions with  $\kappa > 1$ , and in turn (2.9) cannot hold for any  $\mu > 0$ . The contradiction completes the proof.

### §2.5. Proof of Theorem 1.10

We act similarly to §2.3, starting with the lower bound in (1.16). Since, by (1.12),  $\varphi_v(x)$  differs from  $\tilde{\theta}_v(x)$  only by a constant, Lemma 2.1 shows that on  $(v, +\infty)$ , the function  $\mathcal{F}_{\varphi_v,0}$  satisfies the Schrödinger equation

$$\mathcal{F}_{\varphi_v,0}''(x) + \mathcal{V}_{\varphi_v}(x) \mathcal{F}_{\varphi_v,0}(x) = 0,$$

with the potential

$$\mathcal{V}_{\varphi_v}(x) = \mathcal{V}_{\tilde{\theta}_v}(x), \quad (2.13)$$

see (2.7).

We want to apply Theorem 2.5 with

$$g(x) = \varphi_v(x), \quad h(x) = \varphi_v(x), \quad a = v.$$

By (2.5), (2.13), and (2.7),

$$\mathcal{V}_{\varphi_v}(x) - \mathcal{V}_{\varphi_v}(x) = \frac{4v^2 + 3x^2}{4(x^2 - v^2)^2} > 0 \quad \text{for all } x > v,$$

thus verifying condition (C<sub>2</sub>) of Theorem 2.5. Further, by (1.5) and (1.13),

$$\varphi_v(x) - \varphi_v(x) = \frac{3}{8x} + O(x^{-2}) \quad \text{as } x \rightarrow +\infty,$$

confirming that condition  $(C'_3)$  holds with  $s = 1$ . Thus, Theorem 2.5 is applicable and yields the lower bound in (1.16).

Before proving the upper bound in (1.16) in full generality, we will prove it for sufficiently large  $x$  by showing that

$$\varphi_\nu(x) < \tilde{\varphi}_\nu(x) \quad \text{for } x > x_\nu^*. \quad (2.14)$$

Once this is done, the full bound follows easily: firstly, since  $\varphi'_\nu(x_\nu^*) > 0 = \tilde{\varphi}'_\nu(x_\nu^*)$ , the strict inequality also holds for  $x = x_\nu^*$ ; the rest follows since  $\varphi_\nu(x) < \varphi_\nu(x_\nu^*)$  and  $\tilde{\varphi}_\nu(x) > \tilde{\varphi}_\nu(x_\nu^*) = z_\nu^*$  for  $x \in (\nu, x_\nu^*)$ .

We will prove (2.14) by applying Theorem 2.5 with

$$g(x) = \varphi_\nu(x), \quad h(x) = \tilde{\varphi}_\nu(x), \quad a = x_\nu^*.$$

Since  $\tilde{\varphi}'_\nu(x) > 0$  for  $x \in (x_\nu^*, +\infty)$  by Lemma 1.8, we can apply Lemma 2.1 on this interval to deduce that the function  $\mathcal{F}_{\tilde{\varphi}_\nu, 0}$  satisfies there the Schrödinger equation

$$\mathcal{F}_{\tilde{\varphi}_\nu, 0}''(x) + \mathcal{V}_{\tilde{\varphi}_\nu}(x)\mathcal{F}_{\tilde{\varphi}_\nu, 0}(x) = 0,$$

where the potential  $\mathcal{V}_{\tilde{\varphi}_\nu}(x)$  is given by (A.4)–(A.6).

In order to verify condition  $(C_2)$ , we set

$$\delta_\nu(x) := 4096x^2(x^2 - \nu^2)^{10}(\tilde{\varphi}'_\nu(x))^2(\mathcal{V}_{\varphi_\nu}(x) - \mathcal{V}_{\tilde{\varphi}_\nu}(x)).$$

Since the first three factors in the definition of  $\delta_\nu(x)$  are positive for  $x > x_\nu^*$ , it is enough to show that

$$\delta_\nu(x) > 0 \quad \text{for all } x > x_\nu^* \quad (2.15)$$

to ensure that  $(C_2)$  holds. Explicit computation gives

$$\begin{aligned} \delta_\nu(x) = & 4032x^{18} + 16(1208\nu^2 + 27)x^{16} - (158656\nu^4 + 2640\nu^2 + 81)x^{14} \\ & + 16\nu^2(20272\nu^4 + 701\nu^2 - 27)x^{12} - 16\nu^4(12796\nu^4 + 1415\nu^2 + 54)x^{10} \\ & - 64\nu^6(2338\nu^4 - 337\nu^2 + 12)x^8 + 64\nu^8(4543\nu^4 - 164\nu^2 - 4)x^6 \\ & - 3584\nu^{12}(41\nu^2 - 1)x^4 + 1024\nu^{14}(17\nu^2 - 1)x^2 + 4096\nu^{18}, \end{aligned}$$

and we will verify (2.15) separately in two cases.

**Case  $\nu = 0$ .** Since  $x_0^* = \sqrt{\frac{3}{8}}$  and

$$x^{-14}\delta_0(x)\Big|_{x=\sqrt{\frac{3}{8}+\xi}} = 72(56\xi^2 + 48\xi + 9) > 0 \quad \text{for } \xi > 0,$$

(2.15) follows.

**Case  $\nu > 0$ .** We introduce the new variable  $\zeta > 0$  via  $x = \nu(1 + \zeta)$ , and note that

$$\begin{aligned} \nu^{-14}\delta_\nu(x) = & 64\zeta^6(\zeta + 2)^6(63\zeta^6 + 378\zeta^5 + 1625\zeta^4 + 3980\zeta^3 + 5681\zeta^2 + 4410\zeta + 1463)\nu^4 \\ & + 16\zeta^3(\zeta + 1)^2(\zeta + 2)^3 \\ & \times (27\zeta^8 + 216\zeta^7 + 672\zeta^6 + 1008\zeta^5 + 998\zeta^4 + 1304\zeta^3 + 1672\zeta^2 + 1120\zeta + 343)\nu^2 \\ & - (\zeta + 1)^6(3\zeta^2 + 6\zeta + 7)^4, \end{aligned}$$

and, since the coefficient of the  $\nu^2$ -term above is always positive,

$$\begin{aligned} \nu^{-14}\delta_\nu(x) \geq & 64\zeta^6(\zeta + 2)^6(63\zeta^6 + 378\zeta^5 + 1625\zeta^4 + 3980\zeta^3 + 5681\zeta^2 + 4410\zeta + 1463)\nu^4 \\ & - (\zeta + 1)^6(3\zeta^2 + 6\zeta + 7)^4. \end{aligned} \quad (2.16)$$

On the other hand, we have

$$x > x_v^* \iff v^{-4} p_v(v(1+\zeta)) > 0 \iff v^4 \geq \frac{(\zeta+1)^4(3\zeta(\zeta+2)+7)^2}{64\zeta^6(\zeta+2)^6}.$$

Taking this into account in (2.16), we deduce that for  $x > x_v^*$ ,

$$v^{-14} \delta_v(x) \geq 2(\zeta+1)^4(3\zeta(\zeta+2)+7)^2(\zeta(\zeta+2)(\zeta(\zeta+2)(27\zeta(\zeta+2)+409)+1057)+707) > 0,$$

proving (2.15) in this case as well.

To finish the proof of (2.14) using Theorem 2.5, it remains to check condition  $(C'_3)$ , for which we use (1.5) and (1.14) to deduce

$$\tilde{\varphi}_v(x) - \varphi_v(x) = \frac{21}{128x^3} + O(x^{-4}) \quad \text{as } x \rightarrow +\infty,$$

confirming that condition  $(C'_3)$  holds with  $s = 3$ .

### §3. Derivatives of ultraspherical Bessel functions

#### §3.1. Setup III

Let  $\nu \geq 0, \eta \in \mathbb{R}$ , and let

$$U_{\nu,\eta}(x) := x^{-\eta} J_\nu(x), \quad W_{\nu,\eta}(x) := x^{-\eta} Y_\nu(x)$$

denote the *ultraspherical Bessel functions*. We will be interested in their derivatives

$$U'_{\nu,\eta}(x) = x^{-\eta-1} (xJ'_\nu(x) - \eta J_\nu(x)), \quad W'_{\nu,\eta}(x) = x^{-\eta-1} (xY'_\nu(x) - \eta Y_\nu(x)),$$

in practise usually omitting the factor  $x^{-\eta-1}$ , see Figure 10, and denote by

$$u'_{\nu,\eta,k} \quad \text{and} \quad w'_{\nu,\eta,k}$$

the  $k$ th positive zero of  $U'_{\nu,\eta}(x)$  and  $W'_{\nu,\eta}(x)$ , respectively, with the exception in case  $\eta = \nu$ ,

$$u'_{\nu,\nu,1} := 0.$$

Of course, for  $\eta = 0$  we return to the usual derivatives of Bessel functions and their zeros.

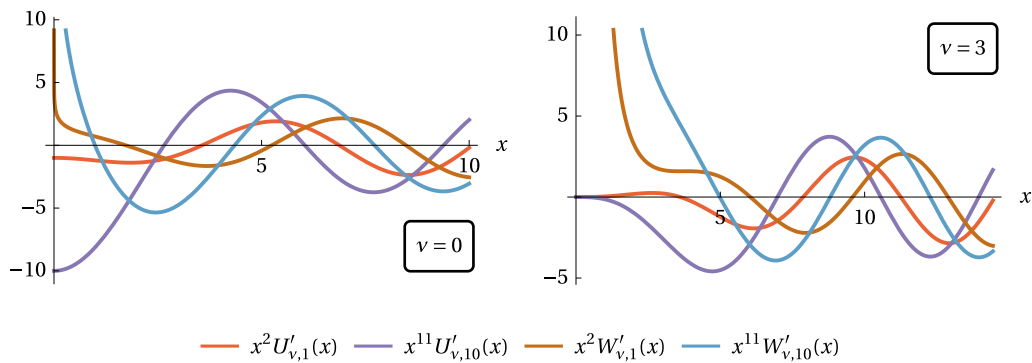


**Figure 10:** Plots of  $x^{\eta+1} U'_{\nu,\eta}(x)$  and  $x^{\eta+1} W'_{\nu,\eta}(x)$ .

The function  $U'_{v,\eta}(x)$  and, specifically, its zeros  $u'_{v,\eta,k}$ , play an important role in spectral geometry. In particular, for  $d \geq 3$ , the numbers

$$\left(u'_{m+\frac{d}{2}-1, \frac{d}{2}-1, k}\right)^2, \quad m \in \mathbb{N} \cup \{0\},$$

are the eigenvalues of multiplicity

$$\binom{m+d-1}{d-1} - \binom{m+d-3}{d-1}$$

of the Neumann Laplacian on the unit ball in  $\mathbb{R}^d$ , see [AB93] and [LMP23, §1.2.3]. Also,

$$\left(u'_{m,\eta,k}\right)^2, \quad m \in \mathbb{N} \cup \{0\},$$

are the non-negative eigenvalues of the Robin Laplacian in the unit disk in  $\mathbb{R}^2$  with the Robin parameter  $-\eta$ , which are taken with multiplicity one if  $m = 0$ , and multiplicity two otherwise, see [BFK16].

For further properties of the derivatives of the ultraspherical Bessel functions and of their roots, including some bounds, see, e.g., [IS88], [LS94], and [L99]. In turn, we are primarily interested in the corresponding phase function which we define and discuss in the next section.

### §3.2. Phase function of ultraspherical Bessel derivatives

As for the standard Bessel functions and their derivatives, we introduce the *modulus* and *phase functions* of the ultraspherical Bessel derivatives,  $L_{v,\eta}, \psi_{v,\eta} : (0, +\infty) \rightarrow \mathbb{R}$  defined by

$$L_{v,\eta}(x) = \sqrt{\left(U'_{v,\eta}(x)\right)^2 + \left(W'_{v,\eta}(x)\right)^2}, \quad U'_{v,\eta}(x) + iW'_{v,\eta}(x) = L_{v,\eta}(x) \left(\cos \psi_{v,\eta}(x) + i \sin \psi_{v,\eta}(x)\right),$$

where we choose a continuous branch of  $\psi_{v,\eta}(x)$  with the initial condition

$$\lim_{x \rightarrow 0^+} \psi_{v,\eta}(x) = \frac{\pi}{2}.$$

Set, for  $v \geq 0$ ,<sup>1</sup>

$$\mu_{v,\eta}^2 = \mu^2 := v^2 - \eta^2,$$

and

$$I_{v,\eta} := \begin{cases} (\mu_{v,\eta}, +\infty) & \text{if } |\eta| < v, \\ (0, +\infty) & \text{if } |\eta| \geq v. \end{cases}$$

We have

**Lemma 3.1.** *Let  $v \geq 0$ ,  $\eta \in \mathbb{R}$ ,  $x > 0$ . If  $\mu_{v,\eta}^2 > 0$ , then the function  $\psi'_{v,\eta}(x)$  has a single zero at  $x = \mu_{v,\eta}$  and is positive for  $x > \mu_{v,\eta}$ , otherwise its derivative is positive on the positive real line. Moreover, on the interval  $I_{v,\eta}$ , the function  $\mathcal{F}_{\psi_{v,\eta},0}(x)$  satisfies the Schrödinger equation (2.2) with the potential*

$$\mathcal{V}_{\psi_{v,\eta}}(x) = 1 - \frac{v^2 - \frac{1}{4}}{x^2} + \frac{2(1-\eta)}{x^2 - \mu_{v,\eta}^2} - \frac{3x^2}{(x^2 - \mu_{v,\eta}^2)^2}.$$

<sup>1</sup>This is a convenient notation as we will not need to consider  $\mu_{v,\eta}$  when  $\mu_{v,\eta}^2$  is negative.

*Proof.* A direct differentiation shows that

$$\psi'_{v,\eta}(x) = \left( \arctan \frac{W'_{v,\eta}(x)}{U'_{v,\eta}(x)} \right)' = \frac{2(x^2 - \mu_{v,\eta}^2)}{\pi x^{2\eta+3} L_{v,\eta}^2(x)}, \quad (3.1)$$

and the first statement then follows immediately since  $L_{v,\eta}(x)$  does not vanish.

Set, for  $x \in I_{v,\eta}$ ,

$$\mathcal{A}_1(x) := \frac{x^{\eta+3/2}}{\sqrt{x^2 - \mu_{v,\eta}^2}} U'_{v,\eta}(x), \quad \mathcal{A}_2(x) := \frac{x^{\eta+3/2}}{\sqrt{x^2 - \mu_{v,\eta}^2}} W'_{v,\eta}(x).$$

A straightforward check shows that we have

$$\mathcal{A}_j''(x) + \left( 1 - \frac{v^2 - \frac{1}{4}}{x^2} + \frac{2(1-\eta)}{x^2 - \mu_{v,\eta}^2} - \frac{3x^2}{(x^2 - \mu_{v,\eta}^2)^2} \right) \mathcal{A}_j(x) = 0, \quad j = 1, 2,$$

and the second statement is obtained by Lemma 2.1.  $\square$

Lemma 3.1 ensures that the inverse function  $(\psi_{v,\eta})^{-1}$  is well-defined on  $[\psi_{v,\eta}(\mu_{v,\eta}), +\infty)$  if  $|\eta| < v$ , or on  $[0, +\infty)$  otherwise, and

$$u'_{v,\eta,k} = (\psi_{v,\eta})^{-1} \left( \pi \left( k - \frac{1}{2} \right) \right), \quad w'_{v,\eta,k} = (\psi_{v,\eta})^{-1}(\pi k). \quad (3.2)$$

We can establish the asymptotics of  $\psi_{v,\eta}(x)$  for large  $x$ .

**Lemma 3.2.** *We have*

$$\begin{aligned} \psi_{v,\eta}(x) &= x - \frac{\pi}{4}(2v-1) + \frac{4v^2 + 3 + 8\eta}{8x} \\ &+ \frac{16v^4 + (192\eta + 184)v^2 - 63 - 128\eta^3 - 192\eta^2 - 144\eta}{384x^3} + O(x^{-5}) \quad \text{as } x \rightarrow +\infty. \end{aligned} \quad (3.3)$$

*Proof.* In essence, we emulate the approach of [HBRV15, §2] to the asymptotics of the standard Bessel phase function. Using standard asymptotics of the Bessel functions and their derivatives [DLMF, §10.17], we get first

$$x^{2\eta} L_{v,\eta}^2(x) = \frac{2}{\pi x} + \frac{8\eta^2 + 8\eta - 4v^2 + 3}{4\pi x^3} + \frac{(4v^2 - 1)(16\eta^2 + 48\eta - 4v^2 + 45)}{64\pi x^5} + O(x^{-7}) \quad \text{as } x \rightarrow +\infty.$$

Computing the reciprocal of this series, substituting it into the right-hand side of the differential equation (3.1), and integrating term by term gives (3.3) except for the  $O(1)$ -term which, at this stage, is an unknown constant of integration  $C$ . Then, in the leading terms,

$$U'_{v,\eta}(x) = L_{v,\eta}(x) \cos \psi_{v,\eta}(x) \sim \sqrt{\frac{2}{\pi}} x^{-\eta-\frac{1}{2}} \cos(x + C),$$

which should match the standard asymptotics

$$U'_{v,\eta}(x) \sim \sqrt{\frac{2}{\pi}} x^{-\eta-\frac{1}{2}} \cos\left(x - \frac{\pi}{4}(2v-1)\right),$$

giving

$$C = -\frac{\pi}{4}(2v-1).$$

$\square$

We are going to demonstrate that the uniform bounds on  $\psi_{v,\eta}(x)$  can be obtained in the same manner as we have done for  $\theta_v(x)$  and  $\varphi_v(x)$ , subject to some restrictions on  $x$ . Generally speaking, such bounds depend upon the signs of  $\eta$  and of  $\mu_{v,\eta}^2$ , so for brevity we from now on restrict ourselves to the case

$$v > \eta > 0 \quad (3.4)$$

(which implies  $\mu_{v,\eta}^2 > 0$ ) and to the lower bound on  $\psi_{v,\eta}(x)$ . See also Remark 3.7 for the case  $v = \eta > 0$ .

### §3.3. Definitions and properties of the auxiliary functions III

Assuming (3.4), we from now on use the shorthand  $\mu$  for  $\mu_{v,\eta} = \sqrt{v^2 - \eta^2}$ . We will keep using indices  $\{v, \eta\}$  for some quantities but  $\{\mu, \eta\}$  for some others where it simplifies the presentation, keeping the relation above in mind.

We define, for  $x > \mu$ , the function

$$\underline{\psi}_{v,\eta}(x) := \sqrt{x^2 - \mu^2} - \left( \frac{\eta^2}{2\mu} + \mu \right) \arccos \frac{\mu}{x} + \frac{\eta}{\sqrt{x^2 - \mu^2}} + \frac{\pi}{4} \left( \frac{\eta^2}{\mu} + 2(\mu - v) + 1 \right). \quad (3.5)$$

*Remark 3.3.* Similarly to Remarks 1.3 and 1.9, the function  $\underline{\psi}_{v,\eta}(x)$  coincides with the two-term asymptotic expansions of  $\psi_{v,\eta}(x)$  in the Debye regime (R<sub>iii</sub>) deduced using the methods of [O74]. ◀

It is obvious that

$$\lim_{x \rightarrow \mu^+} \underline{\psi}_{v,\eta}(x) = \lim_{x \rightarrow +\infty} \underline{\psi}_{v,\eta}(x) = +\infty,$$

and easily checked that

$$\underline{\psi}_{v,\eta}(x) = x - \frac{\pi}{4}(2v - 1) + \frac{v^2 + 2\eta}{2x} + O(x^{-3}) \quad \text{as } x \rightarrow +\infty. \quad (3.6)$$

Further, it is easy to check that its derivative

$$\underline{\psi}'_{v,\eta}(x) = \frac{2x^4 - x^2(\eta(\eta + 2) + 4\mu^2) + \mu^2(\eta^2 + 2\mu^2)}{2x(x^2 - \mu^2)^{3/2}}$$

vanishes at the point

$$x_{\mu,\eta}^{\#} := \frac{1}{2} \sqrt{4\mu^2 + \eta(\eta + 2) + \sqrt{\eta^2(\eta + 2)^2 + 16\mu^2\eta}} > \mu,$$

and is positive for  $x > x_{\mu,\eta}^{\#}$ .

Therefore, the inverse function  $(\underline{\psi}_{v,\eta})^{-1} : (\underline{\psi}_{v,\eta}(x_{\mu,\eta}^{\#}), +\infty) \rightarrow (x_{\mu,\eta}, +\infty)$  is well-defined.

Set additionally, for  $\mu \geq 0, \eta > 0$ ,

$$\begin{aligned} r_{\mu,\eta}(x) := & 12x^{14} \\ & + x^{12}(-44\mu^2 + 4\eta(\eta^3 + 4\eta^2 - 5\eta - 18)) \\ & + x^{10}(40\mu^4 + 8(-3\eta^3 - 10\eta^2 + 6\eta + 5)\eta\mu^2 - \eta^2(\eta + 2)^2(4\eta^2 + 8\eta - 3)) \\ & + x^8(40\mu^6 + 4(15\eta^3 + 40\eta^2 + 2\eta + 70)\eta\mu^4 \\ & \quad + (20\eta^4 + 96\eta^3 + 147\eta^2 + 96\eta + 52)\eta^2\mu^2 + (\eta + 2)^4\eta^4) \\ & + x^6(-100\mu^8 - 8\eta(10\eta^3 + 20\eta^2 + 14\eta + 45)\mu^6 \\ & \quad - \eta^2(40\eta^4 + 144\eta^3 + 171\eta^2 + 116\eta + 80)\mu^4 - 4\eta^5(\eta + 2)^3\mu^2) \\ & + x^4(68\mu^{10} + 4(15\eta^3 + 20\eta^2 + 27\eta + 20)\eta\mu^8 \\ & \quad + (40\eta^4 + 96\eta^3 + 81\eta^2 + 24\eta + 16)\eta^2\mu^6 + 6(\eta + 2)^2\eta^6\mu^4) \\ & + x^2(-16\mu^{12} - 8\eta(3\eta^3 + 2\eta^2 + 4\eta - 4)\mu^{10} - 4\eta^3(5\eta^3 + 6\eta^2 + 3\eta - 4)\mu^8 - 4\eta^7(\eta + 2)\mu^6) \\ & + (4\eta^4\mu^{12} + 4\eta^6\mu^{10} + \eta^8\mu^8), \end{aligned} \quad (3.7)$$

and let  $x_{\mu,\eta}^{\textcircled{a}}$  be the greatest positive real root of (3.7). It exists due to

**Lemma 3.4.** For any  $\mu \geq 0, \eta > 0$ ,

$$x_{\mu,\eta}^{\textcircled{a}} > x_{\mu,\eta}^{\#}.$$

*Proof.* Since the polynomial (3.7) has a positive leading term  $12x^{14}$ , it is sufficient to show that  $r_{\mu,\eta}(x_{\mu,\eta}^{\#}) < 0$ . With the shorthand  $\rho := \sqrt{\eta^2(\eta+2)^2 + 16\mu^2\eta} > 0$ , we get

$$\begin{aligned} r_{\mu,\eta}(x_{\mu,\eta}^{\#}) &= -\frac{3}{16}\eta^2(\eta(\eta+2)^2 + 16\mu^2) \\ &\quad \times (\eta^9 + 10\eta^8 + \eta^7(4\mu^2 + \rho + 40) + 4\eta^6(13\mu^2 + 2\rho + 20) + 4\eta^5(\mu^4 + \mu^2(\rho + 54) + 6\rho + 20) \\ &\quad + 4\eta^4(22\mu^4 + \mu^2(9\rho + 92) + 8(\rho + 1)) + 4\eta^3(\mu^4(\rho + 96) + 8\mu^2(3\rho + 7) + 4\rho) \\ &\quad + 16\eta^2(3\mu^6 + \mu^4(3\rho + 28) + 5\mu^2\rho) + 32\eta(7\mu^6 + 3\mu^4\rho) + 16\mu^6\rho) < 0 \end{aligned}$$

as required.  $\square$

### §3.4. Main results III: bounding the phase and zeros of derivatives of ultraspherical Bessel functions

**Theorem 3.5.** For every  $\nu > \eta > 0$  and every  $x > x_{\mu,\eta}^{\textcircled{a}}$ , with  $\mu = \mu_{\nu,\eta}$ , we have

$$\underline{\psi}_{\nu,\eta}(x) < \psi_{\nu,\eta}(x).$$

Recalling (3.2), we deduce

**Corollary 3.6.** For  $\nu > \eta > 0$ , we have the following bounds, valid for all  $k \in \mathbb{N}$  such that the argument of the inverse function exceeds  $\underline{\psi}_{\nu,\eta}(x_{\mu,\eta}^{\textcircled{a}})$ .

(i)

$$u'_{\nu,\eta,k} < (\underline{\psi}_{\nu})^{-1}\left(\pi\left(k - \frac{1}{2}\right)\right).$$

(ii)

$$w'_{\nu,\eta,k} < (\underline{\psi}_{\nu})^{-1}(\pi k).$$

*Remark 3.7.* Formally, Theorem 3.5 and Corollary 3.6 are inapplicable when  $\eta = \nu$ , and therefore  $\mu = 0$ , since in that case the definition (3.5) does not make sense. If, however, we set, for  $\nu > 0$  and  $x > 0$ ,

$$\underline{\psi}_{\nu,\nu}(x) := \lim_{\eta \rightarrow \nu^-} \underline{\psi}_{\nu,\eta}(x) = x - \frac{\pi}{4}(2\nu - 1) + \frac{\nu(\nu + 2)}{2x},$$

both results become valid for  $\eta = \nu$  without further modifications.  $\blacktriangleleft$

For an illustration of the results in Theorem 3.5, Corollary 3.6, and Remark 3.7, see Figure II.

*Proof of Theorem 3.5.* We will prove (2.14) by applying Theorem 2.5 with

$$g(x) = \underline{\psi}_{\nu,\eta}(x), \quad h(x) = \psi_{\nu,\eta}(x), \quad a = x_{\mu,\eta}^{\textcircled{a}}.$$

Both functions  $g$  and  $h$  have positive derivatives on  $(a, +\infty)$  by Lemma 3.1 and analysis at the beginning of §3.3 (since  $x_{\mu,\eta}^{\textcircled{a}} > x_{\mu,\eta}^{\#} > \mu$ ) and tend to infinity at infinity. We can apply Lemma 2.1 on this interval to deduce that the function  $\mathcal{F}_{\underline{\psi}_{\nu,\eta},0}$  satisfies there the Schrödinger equation

$$\mathcal{F}''_{\underline{\psi}_{\nu,\eta},0}(x) + \mathcal{V}_{\underline{\psi}_{\nu,\eta}}(x)\mathcal{F}_{\underline{\psi}_{\nu,\eta},0}(x) = 0,$$

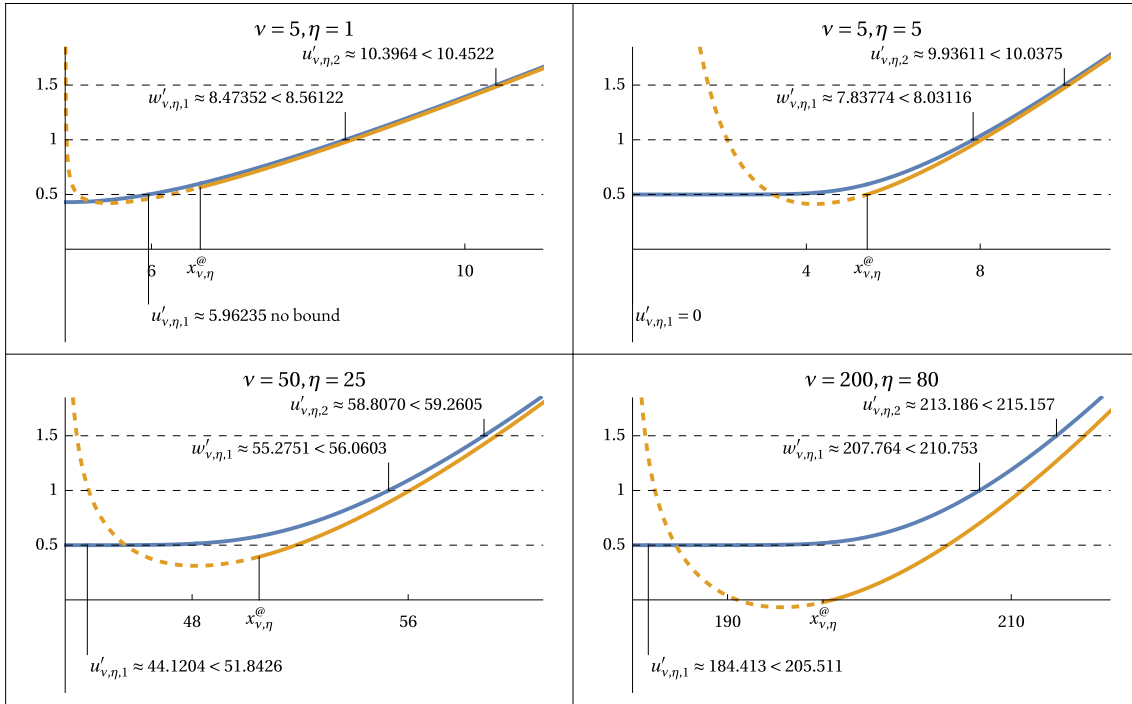


**Figure 11:** All plots show the scaled phase function  $\frac{1}{\pi}\psi_\nu(x)$  (blue), and its scaled bound  $\frac{1}{\pi}\underline{\psi}_\nu(x)$  (orange). The quality of the bounds for  $u'_{\nu,\eta,k}$  and  $w'_{\nu,\eta,k}$  increases with  $k$ .

with the potential  $\mathcal{V}_{\psi_{\nu,\eta}}(x)$  given by (A.7)–(A.9).

An explicit calculation yields

$$16x^4(x^2 - \mu^2)^6 \left( \underline{\psi}'_{\nu,\eta}(x) \right)^2 \left( \mathcal{V}_{\underline{\psi}_{\nu,\eta}}(x) - \mathcal{V}_{\psi_{\nu,\eta}}(x) \right) = r_{\mu,\eta}(x),$$

where the right-hand side is given by (3.7). Since  $r_{\mu,\eta}(x) > 0$  for  $x > a$ , we have verified condition (C<sub>2</sub>) of Theorem 2.5.

Condition (C<sub>3</sub><sup>l</sup>) holds with  $s = 1$  since by (3.3) and (3.6),

$$\psi_{\nu,\eta}(x) - \underline{\psi}_{\nu,\eta}(x) = \frac{3}{8x} + O(x^{-3}) \quad \text{as } x \rightarrow +\infty.$$

□

### §4. Benchmarking and conclusions

In order to set up comparison with previous bounds, we denote

$$\begin{aligned} A_v^{(1)}(\beta) &:= \beta, \\ A_v^{(2)}(\beta) &:= \beta - \frac{4v^2 - 1}{8\beta}, \\ A_v^{(3)}(\beta) &:= \beta - \frac{4v^2 - 1}{8\beta} - \frac{4(4v^2 - 1)(28v^2 - 31)}{3(8\beta)^3}. \end{aligned}$$

and let

$$\beta_{v,k} := \pi \left( k + \frac{v}{2} - \frac{1}{4} \right).$$

The  $i$ -term McMahon asymptotic expansion for the large zeros of the Bessel function of a *fixed* order  $v \geq 0$ , is given, for  $i = 1, 2, 3$ , by the formula

$$j_{v,k} = A_v^{(i)}(\beta_{v,k}) + O(\beta_{v,k}^{-2i+1}) \quad \text{as } k \rightarrow +\infty, \quad (4.1)$$

see [M94], [W95, §15.53], [DLMF, (10.21.19)], and also [N21, Appendix A] for further terms. The remainder term may be alternatively written as  $O(k^{-2(i-1)})$ . The more general asymptotic formulae for  $c_{v,\tau,k}$  are obtained in the same manner by replacing  $\beta_{v,k}$  with  $\pi(k + \frac{v}{2} + \tau - \frac{5}{4})$ .

We have Hethcote's upper bound [He70]:

$$j_{v,k} \leq \begin{cases} A_v^{(2)}(\beta_{v,k}) & \text{if } v \leq \frac{1}{2}, \\ A_v^{(1)}(\beta_{v,k}) & \text{if } v > \frac{1}{2}, \end{cases} =: \tilde{h}_{v,k} \quad \text{for all } v \geq 0 \text{ and } k \in \mathbb{N}.$$

In the same paper, Hethcote also proves the lower bound (but only valid for small  $v$ ),

$$j_{v,k} \geq H_v^{(1)}(\beta_{v,k}) =: \underline{h}_{v,k} \quad \text{for all } 0 \leq v \leq \frac{1}{2} \text{ and } k \in \mathbb{N}.$$

Some improvements of Hethcote's bounds were obtained in [EL00]. Namely, they proved the upper bound

$$j_{v,k} \leq \begin{cases} A_v^{(2)}(\beta_{v,k}) & \text{if } v \leq \frac{1}{2}, \\ A_v^{(3)}(\beta_{v,k}) & \text{if } v > \frac{1}{2}, \end{cases} =: \tilde{\ell}_{v,k} \quad \text{for all } v \geq 0 \text{ and } k \in \mathbb{N}.$$

and the lower bound (for a slightly wider range of  $v$ s)

$$j_{v,k} \geq \begin{cases} A_v^{(3)}(\beta_{v,k}) & \text{if } v \leq \frac{1}{2}, \\ A_v^{(2)}(\beta_{v,k}) & \text{if } \frac{1}{2} < v < \sqrt{\frac{31}{28}}, \end{cases} =: \underline{\ell}_{v,k} \quad \text{for all } 0 \leq v < \sqrt{\frac{31}{28}} \text{ and } k \in \mathbb{N}.$$

For further improvements of these bounds when  $v \leq \frac{1}{2}$ , see [N21].

We note that we always have (when the bounds exist)

$$\underline{h}_{v,k} \leq \underline{\ell}_{v,k} < j_{v,k} < \tilde{\ell}_{v,k} \leq \tilde{h}_{v,k}. \quad (4.2)$$

Alternative bounds, based on the asymptotics of  $j_{v,k}$  in the regime  $(R_{ii})$ , were given by Qu and Wong [QW96]. Let

$$(0 >) a_1 > a_2 > \dots$$

denote the sequence of negative zeros of the Airy function  $\text{Ai}(x)$ . Then

$$\underline{q}_{v,k} := v - a_k \left( \frac{v}{2} \right)^{1/3} < j_{v,k} < v - a_k \left( \frac{v}{2} \right)^{1/3} + \frac{3}{20} a_k^2 \left( \frac{v}{2} \right)^{-1/3} =: \tilde{q}_{v,k} \quad \text{for all } v > 0 \text{ and } k \in \mathbb{N}. \quad (4.3)$$

Switching to existing bounds for  $j'_{\nu,k}$ , we note that although the McMahon asymptotic expansion for these zeros for a fixed  $\nu$  and large  $k$ , similar to (4.1), is well-known, see [DLMF, (10.21.20)], we failed to find any analogues of (4.2) in this case. There is an analogue of the upper bound in (4.3): if

$$(0 >) a'_1 > a'_2 > \dots$$

denotes the sequence of negative zeros of the derivative of the Airy function  $\text{Ai}'(x)$ , then

$$j'_{\nu,k} < \nu + |a'_k| \left( \frac{\nu}{2} + \frac{8|a'_k|^{3/2}}{27} \right)^{1/3} + \frac{9|a'_k|^2}{10 \times 2^{2/3}} \left( 27\nu + 16|a'_k|^{3/2} \right)^{-1/3} =: \tilde{\ell}'_{\nu,k} \quad \text{for all } \nu \geq 0 \text{ and } k \in \mathbb{N},$$

which is obtained from [EL97], [Eoi, §1.7] after some manipulations required by the change of notation.

We compare these bounds to our bounds from Corollaries 1.6 and 1.12 numerically. The results of the computations are collated in Tables 1–3 in Appendix B. We note that all the calculations have been performed with 16 digit precision, and any differences between bounds not exceeding  $10^{-16}$  are ignored. The inverse functions were evaluated using standard `Mathematica` routines with fixed precision.

The upper bound for  $j_{\nu,k}$  obtained by using McMahon's expansions slightly outperforms our bound for low values of  $\nu$  ( $\lesssim 5$ ) and  $k$  ( $\lesssim 100$ ), however even in the worst case  $\nu = \frac{1}{2}$ ,  $k = 1$ , the relative deficiency of our bound is  $7 \times 10^{-4}$ . For a fixed  $\nu$  and very large  $k$ , the bound  $\tilde{\ell}_{\nu,k}$  is theoretically better than our bound  $\tilde{j}_{\nu,k}$ , however in practice the difference is negligible. Similarly, the Airy-type upper bound  $\tilde{q}_{\nu,k}$  should be theoretically better than our bound once one looks deep in the transition region, but in practice within the range of parameters we checked, it outperforms our bound only for very large  $\nu$  and very small  $k$  ( $k \lesssim 10$  for  $\nu = 500000$ ), with the maximal relative deficiency of our bound being  $3 \times 10^{-4}$ : in all other cases our bound is better.

Elbert–Laforgia's lower bound  $\underline{\ell}_{\nu,k}$  generally outperforms our bound  $\underline{j}_{\nu,k}$  (as it is based on an additional term of the asymptotic expansion) but not by much, and is only valid for very low  $\nu$  ( $\lesssim 1$ ). The same observation as in the case of the upper bounds applies to Qu–Wang's lower bound: it becomes slightly more efficient than our bound only for very large  $\nu$  and very small  $k$ .

Concerning the bounds for  $j'_{\nu,k}$ , there is no alternative lower bound to compare with; the upper bound  $\tilde{\ell}'_{\nu,k}$  only performs slightly better than our bound for very small  $k$  and very large  $\nu$ .

Since accurately computing the large zeros of Bessel functions of large order and their derivatives is a non-trivial task, we do not compare our bounds to the actual values of these zeros; instead we plot, in Figures 12 and 13, the *maximal* possible errors by comparing our upper and lower bounds.

### Acknowledgements

Research of NF was supported by the RSF grant 22-11-00092. Research of ML was partially supported by the EPSRC grants EP/W006898/1 and EP/V051881/1, and by the University of Reading RETF Open Fund. Research of IP was partially supported by NSERC.

## References

- [AB93] M. S. Ashbaugh and R. D. Benguria, *Universal bounds for the low eigenvalues of Neumann Laplacians in  $N$  dimensions*. *SIAM J. Math. Anal.* **24**:3 (1993), 557–570. doi: [10.1137/0524034](https://doi.org/10.1137/0524034).  p. 20
- [BR17] J. Bremer, *On the numerical calculation of the roots of special functions satisfying second order ordinary differential equations*. *SIAM J. Sci. Comput.* **39**:1 (2017), A55–A82. doi: [10.1137/16M10571](https://doi.org/10.1137/16M10571).  p. 7
- [BR19] J. Bremer, *An algorithm for the rapid numerical evaluation of Bessel functions of real orders and arguments*. *Adv. Comput. Math.* **45** (2019), 173–211. doi: [10.1007/s10444-018-9613-9](https://doi.org/10.1007/s10444-018-9613-9).  p. 7
- [BR16] J. Bremer and V. Rokhlin, *Improved estimates for nonoscillatory phase functions*. *Discrete Contin. Dyn. Syst. Ser. A* **36**:8 (2016), 4101–4131. doi: [10.3934/dcds.2016.36.4101](https://doi.org/10.3934/dcds.2016.36.4101).  p. 7
- [BFK16] D. Bucur, P. Freitas, and J. Kennedy, *The Robin problem*, in *Shape optimization and spectral theory*, A. Henrot (ed.). De Gruyter Open Poland, 2017. doi: [10.1515/9783110550887-004](https://doi.org/10.1515/9783110550887-004).  p. 20
- [DLMF] *NIST Digital Library of Mathematical Functions*. <https://dlmf.nist.gov/>, release 1.1.11 of 2023-09-15. F. W. J. Olver, A. B. Olde Daalhuis, D. W. Lozier, B. I. Schneider, R. F. Boisvert, C. W. Clark, B. R. Miller, B. V. Saunders, H. S. Cohl, and M. A. McClain (eds.).  pp. 3, 5, 6, 14, 21, 25, and 26
- [CFU57] C. Chester, B. Friedman, and F. Ursell, *An extension of the method of steepest descents*. *Math. Proc. Cambridge Philos. Soc.* **53**:3 (1957), 599–611. doi: [10.1017/S0305004100032655](https://doi.org/10.1017/S0305004100032655).  p. 6
- [Eo1] Á. Elbert, *Some recent results on the zeros of Bessel functions and orthogonal polynomials*. *J. Comput. Appl. Math.* **133** (2001), 65–83. doi: [10.1016/S0377-0427\(00\)00635-X](https://doi.org/10.1016/S0377-0427(00)00635-X).  pp. 7 and 26
- [EL97] Á. Elbert and A. Laforgia, *An upper bound for the zeros of the derivative of Bessel functions*. *Rend. Circ. Mat. Palermo* **46**:1 (1997), 123–130. doi: [10.1007/BF02844477](https://doi.org/10.1007/BF02844477).  pp. 7 and 26
- [ELoo] Á. Elbert and A. Laforgia, *Further results on McMahon’s asymptotic approximations*. *J. Phys. A* **33**:36 (2000), 6333–6341. doi: [10.1088/0305-4470/33/36/305](https://doi.org/10.1088/0305-4470/33/36/305).  pp. 6, 13, 14, and 25
- [FLPS23] N. Filonov, M. Levitin, I. Polterovich, and D. A. Sher, *Pólya’s conjecture for Euclidean balls*. *Invent. Math.* **234** (2023), 129–169. doi: [10.1007/s00222-023-01198-1](https://doi.org/10.1007/s00222-023-01198-1).  pp. 6, 8, and 11
- [FLPS23a] N. Filonov, M. Levitin, I. Polterovich, and D. A. Sher, *Inequalities à la Pólya for the Aharonov–Bohm eigenvalues of the disk*. *arXiv*: [2311.14072](https://arxiv.org/abs/2311.14072).  p. 6
- [GGoo] L. Gatteschi and C. Giordano, *Error bounds for McMahon’s asymptotic approximations of the zeros of the Bessel functions*. *Integral Transforms Spec. Funct.* **10**:1 (2000), 41–56. doi: [10.1080/10652460008819270](https://doi.org/10.1080/10652460008819270).  p. 6
- [GG07] L. Gatteschi and C. Giordano, *On a method for generating inequalities for the zeros of certain functions*. *J. Comput. Appl. Math.* **207**:2 (2007), 186–191. doi: [10.1016/j.cam.2006.10.021](https://doi.org/10.1016/j.cam.2006.10.021).  p. 6
- [HBR15] Z. Heitman, J. Bremer, and V. Rokhlin, *On the existence of nonoscillatory phase functions for second order differential equations in the high-frequency regime*. *J. Comput. Phys.* **290** (2015), 1–27. doi: [10.1016/j.jcp.2015.02.028](https://doi.org/10.1016/j.jcp.2015.02.028).  p. 7
- [HBRV15] Z. Heitman, J. Bremer, V. Rokhlin, and B. Vioreanu, *On the asymptotics of Bessel functions in the Fresnel regime*. *Appl. Comput. Harmon. Anal.* **39**:2 (2015), 347–356. doi: [10.1016/j.acha.2014.12.002](https://doi.org/10.1016/j.acha.2014.12.002).  pp. 7, 13, and 21
- [He70] H. W. Hethcote, *Bounds for zeros of some special functions*. *Proc. Amer. Math. Soc.* **25**:1 (1970), 72–74. doi: [10.2307/2036528](https://doi.org/10.2307/2036528).  pp. 6, 14, and 25
- [Ho17] D. E. Horsley, *Bessel phase functions: calculation and application*. *Numer. Math.* **136** (2017), 679–702. doi: [10.1007/s00211-016-0853-7](https://doi.org/10.1007/s00211-016-0853-7).  pp. 3, 5, 6, 7, 8, 10, and 13

- [IS88] E. K. Ifantis and P. D. Siafarikas, *A differential equation for the positive zeros of the function  $\alpha J_\nu(z) + \gamma z J'_\nu(z)$* . *Z. Analysis Anwend.* **7**:2 (1988), 195–192. doi: [10.4171/ZAA/295](https://doi.org/10.4171/ZAA/295).  p. 20
- [L99] L. J. Landau, *Ratios of Bessel functions and roots of  $\alpha J_\nu(x) + x J'_\nu(x) = 0$* . *J. Math. Anal. Appl.* **240**:1 (1999), 174–204. doi: [10.1006/jmaa.1999.6608](https://doi.org/10.1006/jmaa.1999.6608).  p. 20
- [L31] R. E. Langer, *On the asymptotic solutions of ordinary differential equations, with an application to the Bessel functions of large order*. *Trans. Amer. Math. Soc.* **33**:1 (1931), 23–64. doi: [10.1090/S0002-9947-1931-1501574-0](https://doi.org/10.1090/S0002-9947-1931-1501574-0).  p. 6
- [LMP23] M. Levitin, D. Mangoubi, and I. Polterovich, *Topics in Spectral Geometry*. Graduate Studies in Mathematics **237**. Amer. Math. Soc., Providence, RI, 2023. doi: [10.1090/gsm/237](https://doi.org/10.1090/gsm/237).  p. 20
- [LS94] L. Lorch and P. Szego, *Bounds and monotonicities for the zeros of derivatives of ultraspherical Bessel functions*. *SIAM J. Math. Anal.* **25**:2 (1994), 549–554. doi: [10.1137/S00361410922314](https://doi.org/10.1137/S00361410922314).  p. 20
- [M94] J. McMahon, *On the roots of the Bessel and certain related functions*. *Ann. Math.* **9** (1894/1895), 23–30. doi: [10.2307/1967501](https://doi.org/10.2307/1967501).  p. 25
- [N21] G. Nemes, *Proofs of two conjectures on the real zeros of the cylinder and Airy functions*. *SIAM J. Math. Anal.* **53**:4 (2021), 4328–4349. doi: [10.1137/21M1396794](https://doi.org/10.1137/21M1396794).  pp. 6 and 25
- [O74] F. W. J. Olver, *Asymptotics and Special Functions*. Academic Press, Boston, 1974. doi: [10.1016/C2013-0-11254-8](https://doi.org/10.1016/C2013-0-11254-8).  pp. 8 and 22
- [PA11] T. Pálmai and B. Apagyi, *Interlacing of positive real zeros of Bessel functions*. *J. Math. Anal. Appl.* **375** (2011), 320–322. doi: [10.1016/j.jmaa.2010.09.024](https://doi.org/10.1016/j.jmaa.2010.09.024).  p. 3
- [QW96] C. K. Qu and R. Wong, *“Best possible” upper and lower bounds for the zeros of the Bessel function  $J_\nu(x)$* . *Trans. Amer. Math. Soc.* **351** (1999), 2833–2859. doi: [10.1090/S0002-9947-99-02165-0](https://doi.org/10.1090/S0002-9947-99-02165-0).  pp. 6 and 25
- [S23] D. A. Sher, *Joint asymptotic expansions for Bessel functions*. *Pure Appl. Anal.* **5**:2 (2023), 461–505. doi: [10.2140/paa.2023.5.461](https://doi.org/10.2140/paa.2023.5.461).  pp. 6 and 8
- [W95] G. N. Watson, *A treatise on the theory of Bessel functions*. Second edition. Cambridge Mathematical Library. Cambridge University Press, Cambridge, 1995.  p. 25

### Appendix A. Explicit expressions for some potentials

We have

$$\mathcal{V}_{\varrho_\nu}(x) = \frac{q_\nu^{(1)}(x)}{q_\nu^{(2)}(x)}, \quad (\text{A.1})$$

where

$$\begin{aligned} q_\nu^{(1)}(x) := & 4096x^{24} - 2048(24\nu^2 - 1)x^{22} + 128(2112\nu^4 - 128\nu^2 + 15)x^{20} \\ & - 32(28160\nu^6 - 1760\nu^4 - 584\nu^2 - 1)x^{18} \\ & + (2027520\nu^8 - 107520\nu^6 - 117376\nu^4 + 704\nu^2 + 1)x^{16} \\ & - 16\nu^2(202752\nu^8 - 7680\nu^6 - 13088\nu^4 + 223\nu^2 - 1)x^{14} \\ & + 16\nu^4(236544\nu^8 - 5376\nu^6 - 5000\nu^4 + 585\nu^2 + 6)x^{12} \\ & - 16\nu^6(202752\nu^8 - 2688\nu^6 + 11440\nu^4 + 935\nu^2 - 16)x^{10} \\ & + 16\nu^8(126720\nu^8 - 1920\nu^6 + 15272\nu^4 + 823\nu^2 + 16)x^8 \\ & - 128\nu^{12}(7040\nu^6 - 240\nu^4 + 808\nu^2 + 43)x^6 \\ & + 256(1056\nu^6 - 80\nu^4 + 17\nu^2 + 3)\nu^{14}x^4 \\ & - 1024\nu^{18}(48\nu^4 - 7\nu^2 - 5)x^2 + 1024(4\nu^2 - 1)\nu^{22}, \end{aligned} \quad (\text{A.2})$$

and

$$q_v^{(2)}(x) := 64x^2(x^2 - v^2)^5(8x^6 + (1 - 24v^2)x^4 + 4v^2(6v^2 + 1)x^2 - 8v^6)^2. \quad (\text{A.3})$$

Also,

$$\mathcal{V}_{\tilde{\varphi}_v}(x) = \frac{q_v^{(3)}(x)}{q_v^{(4)}(x)}, \quad (\text{A.4})$$

where

$$\begin{aligned} q_v^{(3)}(x) := & 4096x^{24} - 6144(8v^2 + 1)x^{22} + 128(2112v^4 + 320v^2 - 9)x^{20} \\ & - 32(28160v^6 + 2848v^4 + 760v^2 + 27)x^{18} \\ & + 3(675840v^8 - 3072v^6 + 46208v^4 + 448v^2 + 27)x^{16} \\ & - 16v^2(202752v^8 - 29184v^6 + 16352v^4 + 575v^2 - 27)x^{14} \\ & + 16v^4(236544v^8 - 69888v^6 + 10360v^4 + 1657v^2 + 54)x^{12} \\ & - 48v^6(67584v^8 - 29568v^6 - 1904v^4 + 533v^2 - 16)x^{10} \\ & + 16v^8(126720v^8 - 69504v^6 - 11480v^4 + 479v^2 + 16)x^8 \\ & - 128v^{12}(7040v^6 - 4272v^4 - 632v^2 + 5)x^6 \\ & + 768v^{14}(352v^6 - 208v^4 - v^2 + 1)x^4 \\ & - 1024v^{18}(48v^4 - 23v^2 + 5)x^2 + 1024(4v^2 - 1)v^{22} \end{aligned} \quad (\text{A.5})$$

and

$$q_v^{(4)}(x) := 64x^2(x^2 - v^2)^5(8x^6 - 3(8v^2 + 1)x^4 + 4(6v^2 - 1)v^2x^2 - 8v^6)^2. \quad (\text{A.6})$$

Finally,

$$\mathcal{V}_{\underline{\psi}_{v,\eta}}(x) = \frac{q_{\mu,\eta}^{(5)}(x)}{q_{\mu,\eta}^{(6)}(x)}, \quad \mu = \mu_{v,\eta}, \quad (\text{A.7})$$

where

$$\begin{aligned} q_{\mu,\eta}^{(5)}(x) := & 16x^{16} \\ & - 32x^{14}(\eta^2 + 2\eta + 4\mu^2) \\ & + 8x^{12}(3\eta^4 + 12\eta^3 + \eta^2(28\mu^2 + 9) + 6\eta(8\mu^2 - 1) + (56\mu^2 - 3)\mu^2) \\ & - 4x^{10}(2\eta^6 + 12\eta^5 + 12\eta^4(3\mu^2 + 2) + 8\eta^3(15\mu^2 + 2) \\ & \quad + 14\eta^2(12\mu^2 + 5)\mu^2 + 12\eta(20\mu^2 - 1)\mu^2 + (224\mu^2 - 31)\mu^4) \\ & + x^8(\eta^8 + 8\eta^7 + 8\eta^6(5\mu^2 + 3) + 32\eta^5(6\mu^2 + 1) + 2\eta^4(180\mu^4 + 145\mu^2 + 8) \\ & \quad + 48\eta^3(20\mu^2 + 3)\mu^2 + 4\eta^2(280\mu^4 + 99\mu^2 + 6)\mu^2 \\ & \quad + 8\eta(160\mu^2 + 13)\mu^4 + 20(56\mu^2 - 13)\mu^6) \\ & - \mu^2x^6(4\eta^8 + 24\eta^7 + 16\eta^6(5\mu^2 + 3) + 32\eta^5(9\mu^2 + 1) + \eta^4(480\mu^2 + 293)\mu^2 \\ & \quad + \eta^3(960\mu^4 + 76\mu^2) + 4\eta^2(280\mu^4 + 56\mu^2 + 9)\mu^2 \\ & \quad + 120\eta(8\mu^6 + \mu^4) + 56(16\mu^2 - 5)\mu^6) \\ & + \mu^4x^4(6\eta^8 + 24\eta^7 + 8\eta^6(10\mu^2 + 3) + 192\eta^5\mu^2 + 9\eta^4(40\mu^2 + 11)\mu^2 \\ & \quad + 24\eta^3(20\mu^2 - 1)\mu^2 + 4\eta^2(168\mu^4 + 4\mu^2 + 3)\mu^2 \\ & \quad + 24\eta(16\mu^2 - 1)\mu^4 + 32(14\mu^2 - 5)\mu^6) \\ & - \mu^6x^2(4\eta^8 + 8\eta^7 + 40\eta^6\mu^2 + 48\eta^5\mu^2 + \eta^4(144\mu^2 - 1)\mu^2 + 4\eta^3(24\mu^2 - 5)\mu^2 \\ & \quad + 8\eta^2(28\mu^2 - 3)\mu^4 + 8\eta(8\mu^2 - 5)\mu^4 + 4(32\mu^2 - 11)\mu^6) \\ & + \mu^8(\eta^4 + 4\eta^2\mu^2 + 4\mu^4 - \mu^2)(\eta^2 + 2\mu^2)^2 \end{aligned} \quad (\text{A.8})$$

and

$$q_{\mu,\eta}^{(6)}(x) := 4(x^2 - \mu^2)^3 x^2 (2x^4 - x^2((\eta + 2)\eta + 4\mu^2) + \mu^2(\eta^2 + 2\mu^2))^2. \quad (\text{A.9})$$

## Appendix B. Numerical data

### §B.i. Bounds for zeros of Bessel functions

**Table 1:** The comparison of our, Elbert–Laforgia’s, and Qu–Wong’s upper bounds for  $j_{\nu,k}$ . If  $\tilde{m}_{\nu,k} := \min\{\tilde{j}_{\nu,k}, \tilde{\ell}_{\nu,k}, \tilde{q}_{\nu,k}\}$  denotes the best of the three bounds, the coloured entries in each row are those matching it. If  $\tilde{j}_{\nu,k} > \tilde{m}_{\nu,k}$ , the entry in the last column shows the relative deficiency of our bound.

| $\nu$         | $k$    | $\tilde{j}_{\nu,k}$ | $\tilde{\ell}_{\nu,k}$ | $\tilde{q}_{\nu,k}$ | $\frac{\tilde{j}_{\nu,k}}{\tilde{m}_{\nu,k}} - 1$ |
|---------------|--------|---------------------|------------------------|---------------------|---------------------------------------------------|
| 0             | 1      | 2.40810257797209    | 2.40924613788964       |                     |                                                   |
|               | 2      | 5.52043030619282    | 5.52052356422384       |                     |                                                   |
|               | 5      | 14.9309369836999    | 14.9309416805037       |                     |                                                   |
|               | 10     | 30.6346087249255    | 30.6346092684772       |                     |                                                   |
|               | 50     | 156.295034285583    | 156.295034289676       |                     |                                                   |
|               | 100    | 313.374266079643    | 313.374266080151       |                     |                                                   |
|               | 1000   | 3140.80729522508    | 3140.80729522508       |                     |                                                   |
|               | 10000  | 31415.1411417135    | 31415.1411417135       |                     |                                                   |
|               | 100000 | 314158.479961214    | 314158.479961214       |                     |                                                   |
|               | 500000 | 1570795.54139681    | 1570795.54139681       |                     |                                                   |
| $\frac{1}{2}$ | 1      | 3.14376279614743    | 3.14159265358979       | 3.27460318694968    | $7 \times 10^{-4}$                                |
|               | 2      | 6.28345002833208    | 6.28318530717959       | 7.05438435767338    | $4 \times 10^{-5}$                                |
|               | 5      | 15.7079800888803    | 15.7079632679490       | 20.5314460526698    | $1 \times 10^{-6}$                                |
|               | 10     | 31.4159286363346    | 31.4159265358979       | 47.7692005216613    | $7 \times 10^{-8}$                                |
|               | 50     | 157.079632696288    | 157.079632679490       | 368.663088373722    | $1 \times 10^{-10}$                               |
|               | 100    | 314.159265361079    | 314.159265358979       | 908.847335969838    | $7 \times 10^{-12}$                               |
|               | 1000   | 3141.59265358980    | 3141.59265358979       | 18983.1730584802    |                                                   |
|               | 10000  | 31415.9265358979    | 31415.9265358979       | 406099.051081796    |                                                   |
|               | 100000 | 314159.265358979    | 314159.265358979       | 8735498.79115534    |                                                   |
|               | 500000 | 1570796.32679490    | 1570796.32679490       | 74666197.7784502    |                                                   |
| 1             | 1      | 3.83369791861688    | 3.83188486954530       | 3.88890738513848    | $5 \times 10^{-4}$                                |
|               | 2      | 7.01581736210639    | 7.01559818406170       | 7.40285121412499    | $3 \times 10^{-5}$                                |
|               | 5      | 16.4706452289041    | 16.4706302346712       | 19.2321654812515    | $9 \times 10^{-7}$                                |
|               | 10     | 32.1896818843079    | 32.1896799175785       | 42.2854077969397    | $6 \times 10^{-8}$                                |
|               | 50     | 157.862655418487    | 157.862655401933       | 304.378027137110    | $1 \times 10^{-10}$                               |
|               | 100    | 314.943472839851    | 314.943472837767       | 739.711587305586    | $7 \times 10^{-12}$                               |
|               | 1000   | 3142.37793241682    | 3142.37793241682       | 15150.0966962282    |                                                   |
|               | 10000  | 31416.7119221250    | 31416.7119221250       | 322704.803661024    |                                                   |
|               | 100000 | 314160.050755949    | 314160.050755949       | 6935149.13300128    |                                                   |
|               | 500000 | 1570797.11219282    | 1570797.11219282       | 59267801.5559670    |                                                   |

| $\nu$  | $k$              | $\tilde{J}_{\nu,k}$ | $\tilde{\ell}_{\nu,k}$ | $\tilde{q}_{\nu,k}$ | $\frac{\tilde{J}_{\nu,k}}{\tilde{m}_{\nu,k}} - 1$ |
|--------|------------------|---------------------|------------------------|---------------------|---------------------------------------------------|
| 5      | 1                | 8.77372338204280    | 8.83610697727954       | 8.77748993504362    | $2 \times 10^{-12}$                               |
|        | 2                | 12.3388145653858    | 12.3524627245014       | 12.3951530492719    |                                                   |
|        | 5                | 22.2178113198726    | 22.2186275958908       | 22.7567429583036    |                                                   |
|        | 10               | 38.1598700502104    | 38.1599260373733       | 40.6005910616904    |                                                   |
|        | 50               | 164.072787945468    | 164.072787970360       | 216.371205491807    |                                                   |
|        | 100              | 321.189319569572    | 321.189319568987       | 490.990987826608    |                                                   |
|        | 1000             | 3148.65730681305    | 3148.65730681305       | 9115.22066902932    |                                                   |
|        | 10000            | 31422.9947255486    | 31422.9947255486       | 189888.427570357    |                                                   |
|        | 100000           | 314166.333903060    | 314166.333903060       | 4061112.22022502    |                                                   |
| 500000 | 1570803.39537049 | 1570803.39537049    | 34675838.1018364       |                     |                                                   |
| 10     | 1                | 14.4780593618721    | 14.8150624867862       | 14.4776533239189    | $3 \times 10^{-5}$                                |
|        | 2                | 18.4336923418614    | 18.5520743143216       | 18.4562220388682    |                                                   |
|        | 5                | 28.8873862860562    | 28.9021354143944       | 29.1202550857628    |                                                   |
|        | 10               | 45.2315754422830    | 45.2332565697875       | 46.3737266901699    |                                                   |
|        | 50               | 171.711662928231    | 171.711665150058       | 201.823557261092    |                                                   |
|        | 100              | 328.930191596730    | 328.930191681758       | 433.985076544903    |                                                   |
|        | 1000             | 3156.49941795039    | 3156.49941795039       | 7418.61204821241    |                                                   |
|        | 10000            | 31430.8475141856    | 31430.8475141856       | 151546.091220676    |                                                   |
|        | 100000           | 314174.187765333    | 314174.187765334       | 3227144.69490720    |                                                   |
| 500000 | 1570811.24932825 | 1570811.24932825    | 27533441.1155637       |                     |                                                   |
| 50     | 1                | 57.1207457655499    | 62.0041045949062       | 57.1171076805129    | $6 \times 10^{-5}$                                |
|        | 2                | 62.8080187024269    | 66.0949975045479       | 62.8105158914088    |                                                   |
|        | 5                | 76.4370860305146    | 77.8577326931975       | 76.4662469423382    |                                                   |
|        | 10               | 95.8011096962304    | 96.3212070986120       | 95.9542784414793    |                                                   |
|        | 50               | 229.362879678685    | 229.370990348625       | 235.332191927489    |                                                   |
|        | 100              | 388.693660067007    | 388.694258337930       | 414.265541479911    |                                                   |
|        | 1000             | 3218.95877848403    | 3218.95877849964       | 4923.29223763353    |                                                   |
|        | 10000            | 31493.6412674832    | 31493.6412674832       | 91178.9720478066    |                                                   |
|        | 100000           | 314237.015799664    | 314237.015799664       | 1898940.97658646    |                                                   |
| 500000 | 1570874.08041742 | 1570874.08041742    | 16135766.4340724       |                     |                                                   |
| 100    | 1                | 108.840879423458    | 120.880380157578       | 108.836246832758    | $4 \times 10^{-5}$                                |
|        | 2                | 115.739736248993    | 125.037089659834       | 115.740557472041    |                                                   |
|        | 5                | 131.823950776853    | 137.202588450753       | 131.836011607965    |                                                   |
|        | 10               | 153.900272851252    | 156.664768595604       | 153.962599154298    |                                                   |
|        | 50               | 296.335776171518    | 296.471251735914       | 298.929907132201    |                                                   |
|        | 100              | 459.529546576725    | 459.545645439361       | 471.533009349504    |                                                   |
|        | 1000             | 3296.36998972096    | 3296.36999060841       | 4351.04720098391    |                                                   |
|        | 10000            | 31572.0624063796    | 31572.0624063796       | 74207.6309465587    |                                                   |
|        | 100000           | 314315.543686312    | 314315.543686312       | 1515506.03955682    |                                                   |
| 500000 | 1570952.61784671 | 1570952.61784671    | 12831165.2167116       |                     |                                                   |
| 1000   | 1                | 1018.67064844448    | 1180.40361331412       | 1018.66088584526    | $1 \times 10^{-5}$                                |
|        | 2                | 1032.76258530442    | 1184.62569023296       | 1032.76190059904    |                                                   |
|        | 5                | 1064.24453144028    | 1197.25570362592       | 1064.24532031332    |                                                   |
|        | 10               | 1104.92859950901    | 1218.18794810042       | 1104.93238865887    |                                                   |
|        | 50               | 1328.95755863688    | 1380.97019620599       | 1329.09301911099    |                                                   |
|        | 100              | 1548.25088464171    | 1575.19750272123       | 1548.90887404113    |                                                   |
|        | 1000             | 4602.53426352435    | 4602.69406661919       | 4723.15283247506    |                                                   |
|        | 10000            | 32970.7713584907    | 32970.7713673585       | 43521.6749153743    |                                                   |
|        | 100000           | 315727.692643526    | 315727.692643526       | 742097.821357475    |                                                   |
| 500000 | 1572366.01973148 | 1572366.01973148    | 6066913.80070566       |                     |                                                   |

| $\nu$  | $k$    | $\tilde{j}_{\nu,k}$     | $\tilde{\ell}_{\nu,k}$ | $\tilde{q}_{\nu,k}$     | $\frac{\tilde{j}_{\nu,k}}{\tilde{m}_{\nu,k}} - 1$ |
|--------|--------|-------------------------|------------------------|-------------------------|---------------------------------------------------|
| 10000  | 1      | 10040.0498904506        | 11775.5007480898       | <b>10040.0290289155</b> | $2 \times 10^{-6}$                                |
|        | 2      | 10070.0511840226        | 11779.7297125815       | <b>10070.0495448888</b> | $2 \times 10^{-7}$                                |
|        | 5      | <b>10136.3963629401</b> | 11792.4129183083       | 10136.3963712851        |                                                   |
|        | 10     | <b>10220.8123677153</b> | 11813.5393327241       | 10220.8126794286        |                                                   |
|        | 50     | <b>10662.8217778127</b> | 11982.0061387084       | 10662.8309577604        |                                                   |
|        | 100    | <b>11065.7962862662</b> | 12191.2634222777       | 11065.8362405931        |                                                   |
|        | 1000   | <b>15491.7628369823</b> | 15760.5279241169       | 15498.3768788958        |                                                   |
|        | 10000  | <b>46032.5838776516</b> | 46034.1806805361       | 47239.3537167537        |                                                   |
|        | 100000 | <b>329714.785384131</b> | 329714.785472800       | 435227.952705537        |                                                   |
|        | 500000 | <b>1586471.98808840</b> | 1586471.98808844       | 3063097.67857318        |                                                   |
| 100000 | 1      | 100086.203733327        | 117726.458311625       | <b>100086.158872022</b> | $4 \times 10^{-7}$                                |
|        | 2      | 100150.672924750        | 117730.687968554       | <b>100150.669387466</b> | $4 \times 10^{-8}$                                |
|        | 5      | 100292.921471816        | 117743.376569896       | <b>100292.921340968</b> | $1 \times 10^{-9}$                                |
|        | 10     | <b>100473.286256924</b> | 117764.523007627       | 100473.286274617        |                                                   |
|        | 50     | <b>101406.591053031</b> | 117933.639180549       | 101406.591867126        |                                                   |
|        | 100    | <b>102242.079713765</b> | 118144.896439004       | 102242.083055865        |                                                   |
|        | 1000   | <b>110674.460043079</b> | 121922.018138173       | 110674.861526695        |                                                   |
|        | 10000  | <b>154926.882893420</b> | 157613.832441531       | 154993.057404632        |                                                   |
|        | 100000 | <b>460333.080262841</b> | 460349.047059410       | 472401.362824375        |                                                   |
|        | 500000 | <b>1724975.77003468</b> | 1724975.79260235       | 2028908.15934764        |                                                   |
| 500000 | 1      | 500147.381239784        | 588619.602430817       | <b>500147.304554046</b> | $2 \times 10^{-7}$                                |
|        | 2      | 500257.570515678        | 588623.832149329       | <b>500257.564469154</b> | $1 \times 10^{-8}$                                |
|        | 5      | 500500.599560184        | 588636.521230963       | <b>500500.599326034</b> | $5 \times 10^{-10}$                               |
|        | 10     | 500808.554185199        | 588657.669454029       | <b>500808.554169543</b> | $3 \times 10^{-11}$                               |
|        | 50     | <b>502398.615413161</b> | 588826.844156947       | 502398.615572073        |                                                   |
|        | 100    | <b>503817.163442824</b> | 589038.284846206       | 503817.164086853        |                                                   |
|        | 1000   | <b>517891.863383625</b> | 592838.985093676       | 517891.932705137        |                                                   |
|        | 10000  | <b>586230.238693899</b> | 630329.382318621       | 586239.210056145        |                                                   |
|        | 100000 | <b>967172.336060185</b> | 972162.043475722       | 968798.233994082        |                                                   |
|        | 500000 | <b>2301668.61976330</b> | 2301748.45319828       | 2362010.29220323        |                                                   |

**Table 2:** The comparison of our, Elbert–Laforgia’s, and Qu–Wong’s lower bounds for  $j_{\nu,k}$ . If  $\tilde{m}_{\nu,k} := \max\{j_{\nu,k}, \ell_{\nu,k}, q_{\nu,k}\}$  denotes the best of the three bounds, the coloured entries in each row are those matching it. If  $j_{\nu,k} < \tilde{m}_{\nu,k}$ , the entry in the last column shows the relative deficiency of our bound.

| $\nu$ | $k$    | $\underline{j}_{\nu,k}$ | $\underline{\ell}_{\nu,k}$ | $\underline{q}_{\nu,k}$ | $\frac{\underline{j}_{\nu,k}}{\underline{m}_{\nu,k}} - 1$ |
|-------|--------|-------------------------|----------------------------|-------------------------|-----------------------------------------------------------|
| 0     | 1      | 2.35619449019234        | <b>2.40307454796724</b>    |                         | $-2 \times 10^{-2}$                                       |
|       | 2      | 5.49778714378214        | <b>5.52003775393840</b>    |                         | $-4 \times 10^{-3}$                                       |
|       | 5      | 14.9225651045515        | <b>14.9309173864480</b>    |                         | $-6 \times 10^{-4}$                                       |
|       | 10     | 30.6305283725005        | <b>30.6346064593785</b>    |                         | $-1 \times 10^{-4}$                                       |
|       | 50     | 156.294234516092        | <b>156.295034268531</b>    |                         | $-5 \times 10^{-6}$                                       |
|       | 100    | 313.373867195582        | <b>313.374266077528</b>    |                         | $-1 \times 10^{-6}$                                       |
|       | 1000   | 3140.80725542640        | <b>3140.80729522508</b>    |                         | $-1 \times 10^{-8}$                                       |
|       | 10000  | 31415.1411377345        | <b>31415.1411417135</b>    |                         | $-1 \times 10^{-10}$                                      |
|       | 100000 | 314158.479960816        | <b>314158.479961214</b>    |                         | $-1 \times 10^{-12}$                                      |
|       | 500000 | 1570795.54139673        | <b>1570795.54139681</b>    |                         | $-5 \times 10^{-14}$                                      |

| $\nu$         | $k$                     | $\underline{j}_{\nu,k}$ | $\underline{\ell}_{\nu,k}$ | $\underline{q}_{\nu,k}$ | $\frac{\underline{j}_{\nu,k}}{\underline{m}_{\nu,k}} - 1$ |
|---------------|-------------------------|-------------------------|----------------------------|-------------------------|-----------------------------------------------------------|
| $\frac{1}{2}$ | 1                       | 3.10119764278657        | <b>3.14159265358979</b>    | 1.97291537167673        | $-1 \times 10^{-2}$                                       |
|               | 2                       | 6.26321689238053        | <b>6.28318530717959</b>    | 3.07524677778333        | $-3 \times 10^{-3}$                                       |
|               | 5                       | 15.7000008117865        | <b>15.7079632679490</b>    | 5.50449056479522        | $-5 \times 10^{-4}$                                       |
|               | 10                      | 31.4119470742254        | <b>31.4159265358979</b>    | 8.58162293766878        | $-1 \times 10^{-4}$                                       |
|               | 50                      | 157.078836900071        | <b>157.079632679490</b>    | 24.4517345853548        | $-5 \times 10^{-6}$                                       |
|               | 100                     | 314.158867471034        | <b>314.159265358979</b>    | 38.5846145963924        | $-1 \times 10^{-6}$                                       |
|               | 1000                    | 3141.59261380106        | <b>3141.59265358979</b>    | 177.538763621880        | $-1 \times 10^{-8}$                                       |
|               | 10000                   | 31415.9265319191        | <b>31415.9265358979</b>    | 822.364431896465        | $-1 \times 10^{-10}$                                      |
|               | 100000                  | 314159.265358581        | <b>314159.265358979</b>    | 3815.31399222450        | $-1 \times 10^{-12}$                                      |
| 500000        | 1570796.32679482        | <b>1570796.32679490</b> | 11155.0986540527           | $-5 \times 10^{-14}$    |                                                           |
| 1             | 1                       | 3.79443997608576        | <b>3.83149785113210</b>    | 2.85575708148924        | $-1 \times 10^{-2}$                                       |
|               | 2                       | 6.99700190767405        | <b>7.01553182287974</b>    | 4.24460762400316        | $-3 \times 10^{-3}$                                       |
|               | 5                       | 16.4629809123032        | <b>16.4706250109047</b>    | 7.30526300658577        | $-5 \times 10^{-4}$                                       |
|               | 10                      | 32.1857886427175        | <b>32.1896792156545</b>    | 11.1822068564821        | $-1 \times 10^{-4}$                                       |
|               | 50                      | 157.861863506199        | <b>157.862655395975</b>    | 31.1772945855835        | $-5 \times 10^{-6}$                                       |
|               | 100                     | 314.943075932560        | <b>314.943472837017</b>    | 48.9836076071283        | $-1 \times 10^{-6}$                                       |
|               | 1000                    | 3142.37789263802        | <b>3142.37793241682</b>    | 224.054864934569        | $-1 \times 10^{-8}$                                       |
|               | 10000                   | 31416.7119181462        | <b>31416.7119221250</b>    | 1036.48429790625        | $-1 \times 10^{-10}$                                      |
|               | 100000                  | 314160.050755551        | <b>314160.050755949</b>    | 4807.36445023715        | $-1 \times 10^{-12}$                                      |
| 500000        | 1570797.11219274        | <b>1570797.11219282</b> | 14054.9136473700           | $-5 \times 10^{-14}$    |                                                           |
| 5             | 1                       | <b>8.73567022436826</b> |                            | 8.17329997222154        |                                                           |
|               | 2                       | <b>12.3227225053509</b> |                            | 10.5482009934492        |                                                           |
|               | 5                       | <b>22.2113581058685</b> |                            | 15.7818480787321        |                                                           |
|               | 10                      | <b>38.1564401016457</b> |                            | 22.4113288086710        |                                                           |
|               | 50                      | <b>164.072024198901</b> |                            | 56.6024478771247        |                                                           |
|               | 100                     | <b>321.188930139405</b> |                            | 87.0508148429624        |                                                           |
|               | 1000                    | <b>3148.65726711332</b> |                            | 386.418453827333        |                                                           |
|               | 10000                   | <b>31422.9947215707</b> |                            | 1775.65324258109        |                                                           |
|               | 100000                  | <b>314166.333902662</b> |                            | 8223.76760086749        |                                                           |
| 500000        | <b>1570803.39537041</b> |                         | 24036.8542936740           |                         |                                                           |
| 10            | 1                       | <b>14.4363906385824</b> |                            | 13.9981074326327        |                                                           |
|               | 2                       | <b>18.4174021405972</b> |                            | 16.9902952206943        |                                                           |
|               | 5                       | <b>28.8813543155782</b> |                            | 23.5842773511631        |                                                           |
|               | 10                      | <b>45.2284209970154</b> |                            | 31.9368996726856        |                                                           |
|               | 50                      | <b>171.710928343398</b> |                            | 75.0150103064925        |                                                           |
|               | 100                     | <b>328.929810638849</b> |                            | 113.377548781675        |                                                           |
|               | 1000                    | <b>3156.49937834850</b> |                            | 490.557138795412        |                                                           |
|               | 10000                   | <b>31430.8475102086</b> |                            | 2240.88329239253        |                                                           |
|               | 100000                  | <b>314174.187764936</b> |                            | 10364.9983045269        |                                                           |
| 500000        | <b>1570811.24932817</b> |                         | 30288.2390926064           |                         |                                                           |
| 50            | 1                       | <b>57.0601473524213</b> |                            | 56.8366675420313        |                                                           |
|               | 2                       | <b>62.7869087299433</b> |                            | 61.9532366875564        |                                                           |
|               | 5                       | <b>76.4306643187313</b> |                            | 73.2287875234740        |                                                           |
|               | 10                      | <b>95.7981975064759</b> |                            | 87.5115707849523        |                                                           |
|               | 50                      | <b>229.362259920245</b> |                            | 161.174103797040        |                                                           |
|               | 100                     | <b>388.693323896030</b> |                            | 226.773121843061        |                                                           |
|               | 1000                    | <b>3218.95873962660</b> |                            | 871.741148343930        |                                                           |
|               | 10000                   | <b>31493.6412635141</b> |                            | 3864.75676983414        |                                                           |
|               | 100000                  | <b>314237.015799267</b> |                            | 17756.7980286190        |                                                           |
| 500000        | <b>1570874.08041734</b> |                         | 51825.0605560830           |                         |                                                           |

| $\nu$  | $k$              | $\underline{j}_{\nu,k}$ | $\underline{\ell}_{\nu,k}$ | $\underline{q}_{\nu,k}$ | $\frac{\underline{j}_{\nu,k}}{\underline{m}_{\nu,k}} - 1$ |
|--------|------------------|-------------------------|----------------------------|-------------------------|-----------------------------------------------------------|
| 100    | 1                | 108.766857714791        |                            | 108.613661347338        |                                                           |
|        | 2                | 115.714556094408        |                            | 115.060134517028        |                                                           |
|        | 5                | 131.816671193838        |                            | 129.266438364360        |                                                           |
|        | 10               | 153.897155174351        |                            | 147.261617646583        |                                                           |
|        | 50               | 296.335198187589        |                            | 240.070593577088        |                                                           |
|        | 100              | 459.529237380598        |                            | 322.720177265704        |                                                           |
|        | 1000             | 3296.36995170726        |                            | 1135.32897036330        |                                                           |
|        | 10000            | 31572.0624024203        |                            | 4906.29235454301        |                                                           |
|        | 100000           | 314315.543685914        |                            | 22409.1675624942        |                                                           |
| 500000 | 1570952.61784663 |                         | 65332.4886541907           |                         |                                                           |
| 1000   | 1                | 1018.51756702735        |                            | 1018.55757081489        | $-4 \times 10^{-5}$                                       |
|        | 2                | 1032.71211855974        |                            | 1032.44607624003        |                                                           |
|        | 5                | 1064.23092084051        |                            | 1063.05263006586        |                                                           |
|        | 10               | 1104.92325532692        |                            | 1101.82206856482        |                                                           |
|        | 50               | 1328.95687010529        |                            | 1301.77294585584        |                                                           |
|        | 100              | 1548.25058086023        |                            | 1479.83607607128        |                                                           |
|        | 1000             | 4602.53423266599        |                            | 3230.54864934569        |                                                           |
|        | 10000            | 32970.7713546901        |                            | 11354.8429790625        |                                                           |
|        | 100000           | 315727.692643130        |                            | 49063.6445023715        |                                                           |
| 500000 | 1572366.01973140 |                         | 141539.136473700           |                         |                                                           |
| 10000  | 1                | 10039.7229535966        |                            | 10039.9810743263        | $-3 \times 10^{-5}$                                       |
|        | 2                | 10069.9441122528        |                            | 10069.9029522069        |                                                           |
|        | 5                | 10136.3679056193        |                            | 10135.8427735116        |                                                           |
|        | 10               | 10220.8014007353        |                            | 10219.3689967269        |                                                           |
|        | 50               | 10662.8204962035        |                            | 10650.1501030649        |                                                           |
|        | 100              | 11065.7957673197        |                            | 11033.7754878167        |                                                           |
|        | 1000             | 15491.7628066820        |                            | 14805.5713879541        |                                                           |
|        | 10000            | 46032.5838745664        |                            | 32308.8329239253        |                                                           |
|        | 100000           | 329714.785383751        |                            | 113549.983045269        |                                                           |
| 500000 | 1586471.98808833 |                         | 312782.390926064           |                         |                                                           |
| 100000 | 1                | 100085.500689806        |                            | 100086.136613473        | $-6 \times 10^{-6}$                                       |
|        | 2                | 100150.443003779        |                            | 100150.601345170        | $-2 \times 10^{-6}$                                       |
|        | 5                | 100292.860554032        |                            | 100292.664383644        |                                                           |
|        | 10               | 100473.262872899        |                            | 100472.616176466        |                                                           |
|        | 50               | 101406.588375922        |                            | 101400.705935771        |                                                           |
|        | 100              | 102242.078649619        |                            | 102227.201772657        |                                                           |
|        | 1000             | 110674.459991335        |                            | 110353.289703633        |                                                           |
|        | 10000            | 154926.882890391        |                            | 148062.923545430        |                                                           |
|        | 100000           | 460333.080262533        |                            | 323091.675624942        |                                                           |
| 500000 | 1724975.77003461 |                         | 752324.886541907           |                         |                                                           |
| 500000 | 1                | 500146.179459647        |                            | 500147.291537168        | $-2 \times 10^{-6}$                                       |
|        | 2                | 500257.177589753        |                            | 500257.524677778        | $-7 \times 10^{-7}$                                       |
|        | 5                | 500500.495512600        |                            | 500500.449056480        |                                                           |
|        | 10               | 500808.514273685        |                            | 500808.162293767        |                                                           |
|        | 50               | 502398.610860722        |                            | 502395.173458535        |                                                           |
|        | 100              | 503817.161639156        |                            | 503808.461459639        |                                                           |
|        | 1000             | 517891.863298728        |                            | 517703.876362188        |                                                           |
|        | 10000            | 586230.238689636        |                            | 582186.443189646        |                                                           |
|        | 100000           | 967172.336059901        |                            | 881481.399222450        |                                                           |
| 500000 | 2301668.61976324 |                         | 1615459.86540527           |                         |                                                           |

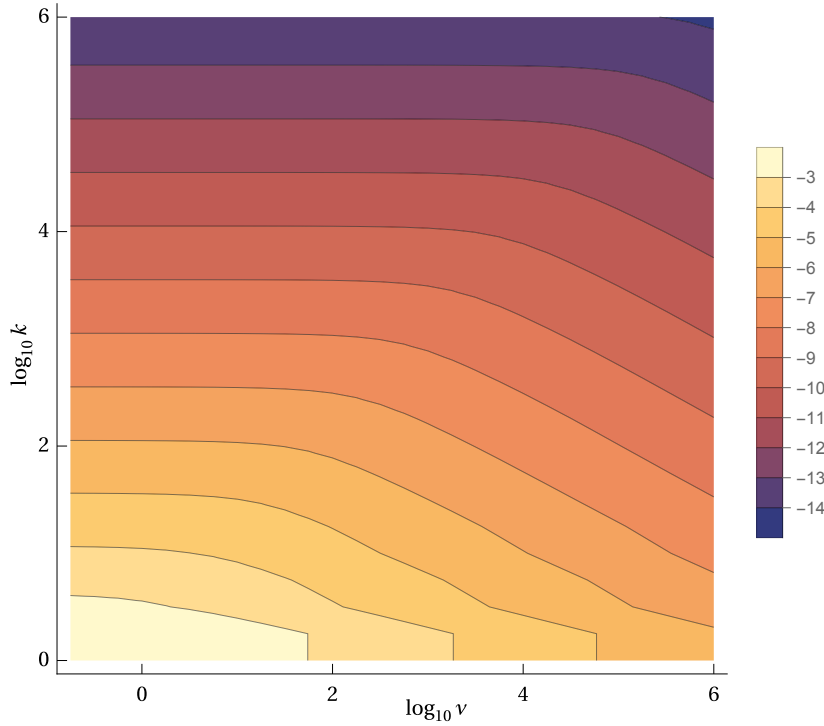


**Figure 12:** The contour plot of  $\log_{10} \left( \frac{\tilde{j}_{v,k}}{j_{v,k}} - 1 \right)$ , which estimates from above the maximum possible order of relative error of our approximations of  $j_{v,k}$ .

**§B.2. Bounds for zeros of derivatives of Bessel functions**

**Table 3:** Our lower bound and the comparison of our and Elbert–Laforgia’s upper bounds for  $j'_{v,k}$ . If  $\tilde{m}'_{v,k} := \min \{ \tilde{j}'_{v,k}, \tilde{\ell}'_{v,k} \}$  denotes the best of the two upper bounds, the coloured entries in each row are those matching it. If  $\tilde{j}'_{v,k} > \tilde{m}'_{v,k}$ , the entry in the last column shows the relative deficiency of our bound.

| $\nu$ | $k$    | $\underline{j}'_{\nu,k}$ | $\tilde{j}'_{\nu,k}$ | $\tilde{\ell}'_{\nu,k}$ | $\frac{\tilde{j}'_{\nu,k}}{\tilde{m}'_{\nu,k}} - 1$ |
|-------|--------|--------------------------|----------------------|-------------------------|-----------------------------------------------------|
| 0     | 2      | 3.82905543678956         | 3.92699081698724     | 5.21994815723788        |                                                     |
|       | 5      | 13.3236232806872         | 13.351768777566      | 17.8482723692095        |                                                     |
|       | 10     | 29.0468218553286         | 29.0597320457056     | 38.8629189129038        |                                                     |
|       | 50     | 154.721014471994         | 154.723438189297     | 206.941758158503        |                                                     |
|       | 100    | 311.801868181958         | 311.803070868787     | 417.036190247476        |                                                     |
|       | 1000   | 3139.23633964380         | 3139.23645909960     | 4198.72872262331        |                                                     |
|       | 10000  | 31413.5703294702         | 31413.5703414077     | 42015.6503274934        |                                                     |
|       | 100000 | 314156.909163295         | 314156.909164489     | 420184.866007090        |                                                     |
|       | 500000 | 1570793.97060017         | 1570793.97060041     | 2100936.93567796        |                                                     |

| $\nu$         | $k$    | $\underline{j}'_{\nu,k}$ | $\tilde{j}'_{\nu,k}$    | $\tilde{\ell}'_{\nu,k}$ | $\frac{\tilde{j}'_{\nu,k}}{\tilde{m}'_{\nu,k}} - 1$ |
|---------------|--------|--------------------------|-------------------------|-------------------------|-----------------------------------------------------|
| $\frac{1}{2}$ | 1      |                          | <b>1.48584693535690</b> | 1.52657094660980        |                                                     |
|               | 2      | 4.60247860677616         | <b>4.68568659322651</b> | 5.84128905032192        |                                                     |
|               | 5      | 14.1016664264204         | <b>14.1283185385025</b> | 18.4716385900913        |                                                     |
|               | 10     | 29.8283630264584         | <b>29.8409412351793</b> | 39.4867451802621        |                                                     |
|               | 50     | 155.505621002290         | <b>155.508032535003</b> | 207.565903087165        |                                                     |
|               | 100    | 312.586869472825         | <b>312.588069144796</b> | 417.660372359456        |                                                     |
|               | 1000   | 3140.02169802843         | <b>3140.02181745436</b> | 4199.35293773371        |                                                     |
|               | 10000  | 31414.3557236548         | <b>31414.3557355921</b> | 42016.2745458797        |                                                     |
|               | 100000 | 314157.694561061         | <b>314157.694562255</b> | 420185.490225804        |                                                     |
|               | 500000 | 1570794.75599825         | <b>1570794.75599849</b> | 2100937.55989670        |                                                     |
| 1             | 1      |                          | 2.11506214188671        | <b>2.11499393987502</b> | $3 \times 10^{-5}$                                  |
|               | 2      | 5.33004070160281         | <b>5.40501381523099</b> | 6.45712461607948        |                                                     |
|               | 5      | 14.8635367796392         | <b>14.8889705581512</b> | 19.0933165595504        |                                                     |
|               | 10     | 30.6019171965764         | <b>30.6141946267452</b> | 40.1097896852094        |                                                     |
|               | 50     | 156.288635764017         | <b>156.291035345361</b> | 208.189900476501        |                                                     |
|               | 100    | 313.371074961794         | <b>313.372271647828</b> | 418.284481220551        |                                                     |
|               | 1000   | 3140.80697683556         | <b>3140.80709623164</b> | 4199.97714556513        |                                                     |
|               | 10000  | 31415.1411098817         | <b>31415.1411218186</b> | 42016.8987635385        |                                                     |
|               | 100000 | 314158.479958031         | <b>314158.479959224</b> | 420186.114444445        |                                                     |
|               | 500000 | 1570795.54139618         | <b>1570795.54139641</b> | 2100938.18411543        |                                                     |
| 5             | 1      | 6.28826192531053         | 6.65074326003913        | <b>6.54714840840174</b> | $2 \times 10^{-2}$                                  |
|               | 2      | 10.5188417338511         | <b>10.5753107094334</b> | 11.2332989986105        |                                                     |
|               | 5      | 20.5754812539651         | <b>20.5957954835809</b> | 24.0099702812020        |                                                     |
|               | 10     | 36.5607736396374         | <b>36.5713809406576</b> | 45.0667270043476        |                                                     |
|               | 50     | 162.498179300523         | <b>162.500490908179</b> | 213.176588124942        |                                                     |
|               | 100    | 319.616768720740         | <b>319.617942511495</b> | 423.274719776078        |                                                     |
|               | 1000   | 3147.08634964664         | <b>3147.08646880501</b> | 4204.97054621798        |                                                     |
|               | 10000  | 31421.4239132894         | <b>31421.4239252240</b> | 42021.8924786219        |                                                     |
|               | 100000 | 314164.763105141         | <b>314164.763106335</b> | 420191.108190953        |                                                     |
|               | 500000 | 1570801.82457384         | <b>1570801.82457408</b> | 2100943.17786473        |                                                     |
| 10            | 1      | 11.6398057744632         | 12.0162638908975        | <b>11.8660736403637</b> | $1 \times 10^{-2}$                                  |
|               | 2      | 16.4468248709150         | <b>16.4994512103844</b> | 16.9720812337165        |                                                     |
|               | 5      | 27.1819924558840         | <b>27.1998893619366</b> | 30.0345337375884        |                                                     |
|               | 10     | 43.6067615870698         | <b>43.6162303330504</b> | 51.1985421323618        |                                                     |
|               | 50     | 170.135218972640         | <b>170.137436706410</b> | 219.396825169749        |                                                     |
|               | 100    | 327.357136966911         | <b>327.358284407731</b> | 429.505960987985        |                                                     |
|               | 1000   | 3154.92845527118         | <b>3154.92857413496</b> | 4211.21164225011        |                                                     |
|               | 10000  | 31429.2767018707         | <b>31429.2767138023</b> | 42028.1345570098        |                                                     |
|               | 100000 | 314172.616967415         | <b>314172.616968609</b> | 420197.350367542        |                                                     |
|               | 500000 | 1570809.67853160         | <b>1570809.67853184</b> | 2100949.42005005        |                                                     |
| 50            | 1      | 52.8187848373174         | 53.3254083348661        | <b>53.0440529190390</b> | $5 \times 10^{-3}$                                  |
|               | 2      | 60.0249962636869         | <b>60.0813194544867</b> | 60.2418339467916        |                                                     |
|               | 5      | 74.3163203933786         | <b>74.3314682956021</b> | 75.7386724516605        |                                                     |
|               | 10     | 93.9425695282024         | <b>93.9498510947580</b> | 98.4545059578280        |                                                     |
|               | 50     | 227.750672604515         | <b>227.752470650764</b> | 268.662409540753        |                                                     |
|               | 100    | 387.108315157524         | <b>387.109313313986</b> | 479.099715011984        |                                                     |
|               | 1000   | 3217.38763707313         | <b>3217.38775367737</b> | 4261.11426459507        |                                                     |
|               | 10000  | 31492.0704532998         | <b>31492.0704652076</b> | 42078.0685658962        |                                                     |
|               | 100000 | 314235.445001727         | <b>314235.445002920</b> | 420247.287518400        |                                                     |
|               | 500000 | 1570872.50962077         | <b>1570872.50962101</b> | 2100999.35748022        |                                                     |

| $\nu$  | $k$              | $\tilde{j}'_{\nu,k}$    | $\tilde{J}'_{\nu,k}$    | $\tilde{\ell}'_{\nu,k}$ | $\frac{\tilde{J}'_{\nu,k}}{\tilde{m}'_{\nu,k}} - 1$ |
|--------|------------------|-------------------------|-------------------------|-------------------------|-----------------------------------------------------|
| 100    | 1                | 103.552648845966        | 104.160029957632        | <b>103.803049301258</b> | $3 \times 10^{-3}$                                  |
|        | 2                | 112.385101849666        | <b>112.448430986771</b> | 112.528002221252        |                                                     |
|        | 5                | 129.358651207261        | <b>129.374174936818</b> | 130.325058224489        |                                                     |
|        | 10               | 151.813259002596        | <b>151.820223347072</b> | 155.042104955214        |                                                     |
|        | 50               | 294.664327855513        | <b>294.665911746948</b> | 329.158665247029        |                                                     |
|        | 100              | 457.918838435071        | <b>457.919731860974</b> | 540.487440358064        |                                                     |
|        | 1000             | 3294.79831773381        | <b>3294.79843173622</b> | 4323.42741287888        |                                                     |
|        | 10000            | 31570.4915863354        | <b>31570.4915982138</b> | 42140.4795335826        |                                                     |
|        | 100000           | 314313.972888315        | <b>314313.972889508</b> | 420309.708302353        |                                                     |
| 500000 | 1570951.04705006 | <b>1570951.04705030</b> | 2101061.77913701        |                         |                                                     |
| 1000   | 1                | 1007.65497214255        | 1008.87692662131        | <b>1008.10741918263</b> | $8 \times 10^{-4}$                                  |
|        | 2                | 1025.97327758496        | 1026.08853535440        | <b>1026.00990668415</b> | $8 \times 10^{-5}$                                  |
|        | 5                | 1059.53767346269        | <b>1059.56146481700</b> | 1059.76655932628        |                                                     |
|        | 10               | 1101.19242597862        | <b>1101.20147226161</b> | 1102.01144720199        |                                                     |
|        | 50               | 1326.56778093642        | <b>1326.56910593182</b> | 1338.72297124053        |                                                     |
|        | 100              | 1546.19139906085        | <b>1546.19204915940</b> | 1582.10105006399        |                                                     |
|        | 1000             | 4600.92489073707        | <b>4600.92497958265</b> | 5433.32953880577        |                                                     |
|        | 10000            | 32969.1998239474        | <b>32969.1998353403</b> | 43262.6382055024        |                                                     |
|        | 100000           | 315726.121837736        | <b>315726.121838924</b> | 421433.158077796        |                                                     |
| 500000 | 1572364.44893452 | <b>1572364.44893476</b> | 2102185.34408437        |                         |                                                     |
| 10000  | 1                | 10016.4918376026        | 10019.0850161927        | <b>10017.4305732935</b> | $2 \times 10^{-4}$                                  |
|        | 2                | 10055.6275626539        | 10055.8663257080        | <b>10055.6423608815</b> | $2 \times 10^{-5}$                                  |
|        | 5                | 10126.5382295259        | <b>10126.5852535008</b> | 10126.5888462274        |                                                     |
|        | 10               | 10213.1216137128        | <b>10213.1385542345</b> | 10213.3033978649        |                                                     |
|        | 50               | 10658.2856359516        | <b>10658.2876108152</b> | 10661.1849966748        |                                                     |
|        | 100              | 11062.1238234066        | <b>11062.1246535611</b> | 11071.3066333350        |                                                     |
|        | 1000             | 15489.7059732163        | <b>15489.7060377999</b> | 15852.5040437567        |                                                     |
|        | 10000            | 46030.9746376957        | <b>46030.9746465753</b> | 54361.7461824340        |                                                     |
|        | 100000           | 329713.213863324        | <b>329713.213864463</b> | 432654.745761900        |                                                     |
| 500000 | 1586470.41726056 | <b>1586470.41726079</b> | 2113418.40311191        |                         |                                                     |
| 100000 | 1                | 100035.530371101        | 100041.098972602        | <b>100037.536956311</b> | $4 \times 10^{-5}$                                  |
|        | 2                | 100119.692630670        | 100120.202625833        | <b>100119.708964190</b> | $5 \times 10^{-6}$                                  |
|        | 5                | 100271.813981416        | 100271.913355254        | <b>100271.825350454</b> | $9 \times 10^{-7}$                                  |
|        | 10               | 100456.883755739        | <b>100456.919097553</b> | 100456.923246477        |                                                     |
|        | 50               | 101397.105043612        | <b>101397.108914265</b> | 101397.740786006        |                                                     |
|        | 100              | 102234.528924186        | <b>102234.530469187</b> | 102236.567493622        |                                                     |
|        | 1000             | 110670.793673338        | <b>110670.793755672</b> | 110763.646675313        |                                                     |
|        | 10000            | 154924.826290601        | <b>154924.826297055</b> | 158556.516370227        |                                                     |
|        | 100000           | 460331.471036162        | <b>460331.471037050</b> | 543645.912187864        |                                                     |
| 500000 | 1724974.19659187 | <b>1724974.19659209</b> | 2225491.96489915        |                         |                                                     |
| 500000 | 1                | 500060.756008294        | 500070.272554347        | <b>500064.182433034</b> | $1 \times 10^{-5}$                                  |
|        | 2                | 500204.624142480        | 500205.494863009        | <b>500204.649221081</b> | $2 \times 10^{-6}$                                  |
|        | 5                | 500464.546806439        | 500464.716136887        | <b>500464.551147341</b> | $3 \times 10^{-7}$                                  |
|        | 10               | 500780.557830912        | 500780.617909442        | <b>500780.571426180</b> | $9 \times 10^{-8}$                                  |
|        | 50               | 502382.483279350        | <b>502382.489781183</b> | 502382.701278916        |                                                     |
|        | 100              | 503804.363624797        | <b>503804.366193259</b> | 503805.063905356        |                                                     |
|        | 1000             | 517885.834593690        | <b>517885.834718306</b> | 517918.417812500        |                                                     |
|        | 10000            | 586227.229833856        | <b>586227.229841076</b> | 587665.712270748        |                                                     |
|        | 100000           | 967170.501022458        | <b>967170.501023138</b> | 1017601.68651123        |                                                     |
| 500000 | 2301667.01053780 | <b>2301667.01053798</b> | 2718242.20552639        |                         |                                                     |

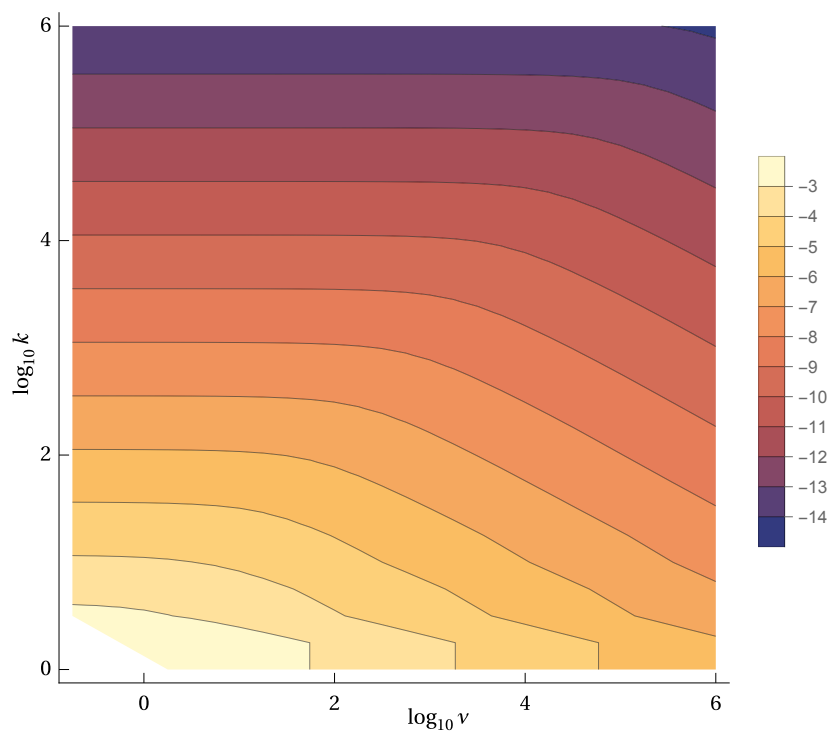


**Figure 13:** The contour plot of  $\log_{10} \left( \frac{\tilde{j}'_{v,k}}{j'_{v,k}} - 1 \right)$ , which estimates from above the maximum possible order of the relative error of our approximations of  $j'_{v,k}$ .